Effects of a Tuned Mass Damper on Wind-Induced Motions in Tall Buildings

by

Julien Carlot

Diplôme d'Ingénieur, Génie Civil Spécialité Bâtiment
Ecole Spéciale des Travaux Publics, 2012

Submitted to the Department of Civil and Environmental Engineering in partial fulfillment of the requirements for the degree of

MASTER OF ENGINEERING IN CIVIL AND ENVIRONMENTAL ENGINEERING
AT THE
MASSACHUSETTS INSTITUTE OF TECHNOLOGY

JUNE 2012

Signature of author: _____
Department of Civil and Environmental Engineering
May 11, 2012

Certified by: _____
Jerome J. Connor
Professor of Civil and Environmental Engineering
Thesis Supervisor

Accepted by: _____
Heidi M. Nepf
Chair, Departmental Committee for Graduate Students

Effects of a Tuned Mass Damper on Wind-Induced Motions in Tall Buildings

by

Julien Carlot

Submitted to the Department of Civil and Environmental Engineering
on May 11, 2012 in Partial Fulfillment of the
Requirements for the Degree of Master of Engineering in
Civil and Environmental Engineering

ABSTRACT

With ever increasing constructability capacities, engineers have found solutions to build taller and taller structures. However, the race for the sky has not only brought up new ways of building, it has also created new problems to face, namely wind-induced motions. In particular, wind loadings are now the source of vibrations in buildings, which have a direct impact on users. While in the past, strength capacities were the main concern, nowadays, human's comfort has become the one of the new primary problems engineers have to face when designing skyscrapers. Several solutions have been developed throughout the years in order to mitigate the response of a building to wind loads, one of which is the Tuned Mass Damper system. This system, which consists of an auxiliary mass added to a structure, significantly reduces motions in high-rise buildings. However, the theory is often based on a harmonic excitation of a building, which is not necessarily the exact representation of wind loads. This paper analyzes the effects of a Tuned Mass Damper on the response of a building to a saw tooth excitation with white noise, which seems to be a better approximation of how wind loads act on tall structures.

Thesis Supervisor: Jerome J. Connor
Title: Professor of Civil and Environmental Engineering

Acknowledgments

First and foremost, I would like to thank my parents for giving me the chance to attend Massachusetts Institute of Technology. I would not have made it this far was it not for their constant support, both moral and financial, and belief in me.

Second, I would like to thank my dearest Julie, for her constant effort throughout the whole year to encourage me. Even though the distance is great between us, she has provided me with the strength to never give up during this challenging year, and has always been there for me, especially during hard times.

I would like to thank Professor Jerome J. Connor for everything that he has taught me throughout this year, as well as for all the guidance he gave me during my studies. His invaluable help has truly made my year at Massachusetts Institute of Technology much easier and entertaining. I am extremely pleased to have been able to share some of his knowledge through the courses of my Master's degree.

I would also like to thank Pierre Ghisbain for his valuable time all year long. His enthusiasm and advice always encouraged me to pursue my work even through hard times. His constant availability and promptness to answer questions have made this year much more enjoyable.

Last I'd like to thank all of the students from the Civil and Environmental Engineering's Master of Engineering Program. Thank you all for having helped me to integrate this new situation with such ease. Discovering and settling in a new country has never been easier and more exciting than with all of you.

Humans have always sought to challenge nature; and building tall structures has always been a way for them to prove their ability to surpass what seemed impossible. Even today, with the recent construction of Burj Khalifa, the tallest structure in the whole world, rising up to 2,716.5 feet, or 828 meters, and comprised of more than 160 stories, humans have shown once again that they can always push further the limits of their capacities. However, in order to build high, we had to come up with new technologies and construction methods, thus updating our way to think about civil engineering. Indeed, one of the major changes in buildings is the change in stiffness of tall structures, which are becoming more and more flexible. One of the key consequences of this evolution is the appearance of new issues we didn't need to take into account before, especially wind-induced motion. Wind load on tall buildings is so particular that it has to be treated specifically for new high-rise structures. In particular, wind loadings are responsible of vibrations in tall buildings, which can sometimes cause motion sickness to building users. Such a scenario is not acceptable, and it is up to engineers to find ways to mitigate building vibrations. Several schemes have been developed since the beginning of the race towards the sky, one of them being the addition of a tuned auxiliary damper at the top of the skyscraper. This paper focuses on the effectiveness of such devices, and simulations will be run to analyze a structure's response to wind load, when mounted with a Tuned Mass Damper system.

Chapter 1 deals with the evolution of tall buildings from past to present, and gives a few figures on the current heights we are technologically capable of attaining. It also gives two examples of recently designed Tuned Mass Dampers, in order for the user to get a rough idea of their properties.

Chapter 2 focuses more on wind-induced motions in tall buildings. It can be divided into three parts: firstly a general discussion about wind and wind loads is given. In a second part, we list and explain a few experiments which have been led to understand how building motions could produce

motion sickness, as well as the thresholds which can cause discomfort. Finally, several possible ways of mitigating wind induced motions are discussed.

In Chapter 3, discussions are led concerning one of these solutions: the Tuned Mass Damper system. The theoretical model is explained in a first part, and then, a list of devices revolving around the Tuned Mass Damper system is presented.

Finally, in Chapter 4, we implement a MATLAB®[1] code in order to simulate the response of a single degree of freedom (DOF) system with a Tuned Mass Damper attached to it. The system is subjected to several types of loading, and results are discussed to confirm the efficiency of such a device.

Chapter 1 - Evolution of High Rise Buildings

1.1 High Buildings in the Ancient Time

1.1.1 Brief History of Tall Monuments and Buildings

Since the beginning of time, buildings and monuments have been a symbol of a man's power. Not only did the structures need to be vast and majestic, but very quickly the height factor was taken into account and made one of the key features of monuments. Height became a major element for two reasons: firstly, in ancient times, religion played a key role in society; hence most of the monuments were built with a religious connotation – burial monuments, places of worship, palace housing a king or queen which was supposedly a representative of God, etc. Since most religions associate gods and the afterlife with the sky and the clouds, building up was a way to symbolically getting closer to them.

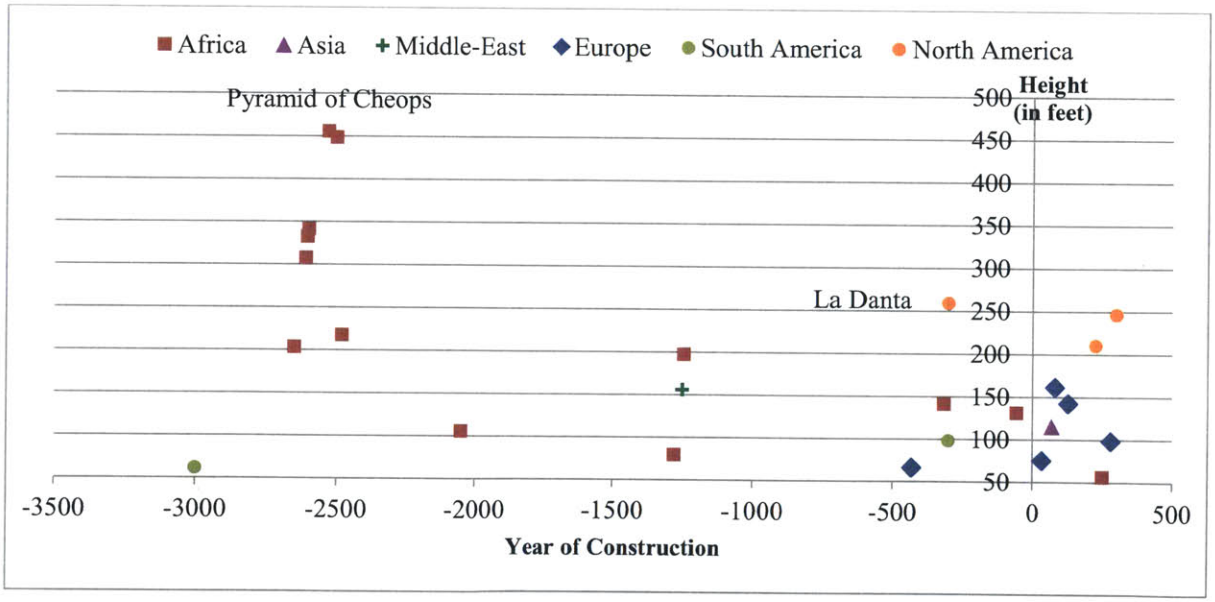

Figure 1.1: List of High Monuments and Buildings Before 500 (Data from [2])

A second, more pragmatic reason was related to sight. Whether those monuments had to be seen in order to help people position themselves (places of cult were meant to attract pilgrims) or

simply to remind surrounding areas of the leader's supremacy (tombs or palaces), building high monuments was a way of making sure everyone could see that symbol of power from afar.

Figure 1.1 shows a list of the tallest buildings and monuments (higher than 50 feet) built according to continent and date of completion, before 500 A.D. As will be discussed later in section 1.2, the tallest monuments built were the Egyptian pyramids – 5 of them being taller than 300 feet. The tallest pyramid (Pyramid of Cheops) remained the tallest structure until the 13th century.

1.1.2 Structure of Old Monuments and Buildings

Different types of high buildings can be seen through history, each having their own different approach on structure.

1.1.2.1 Pyramids

Pyramids were the first buildings that had a significant height to differentiate them from common structures. They are believed to have been first built near 4000 B.C. The most famous ones were used either as temples (Mesopotamian, Mesoamerican) or as tombs (Egypt). Egyptian pyramids are more structurally impressive as they are steeper (taller with a smaller base) than American ones, and the construction was usually shorter – few decades against centuries. The structures of pyramids evolved with time, becoming more and more challenging.

Figure 1.2: Evolution of Pyramid Structures [3]
From left to right: Step Pyramid of Djoser - Bent Pyramid - Gyza Pyramid Complex

As can be seen in Figure 1.2, pyramids' scheme evolved from a stair-like pyramid (Step Pyramid) to a semi straight pyramid (Bent Pyramid), to finally attain a straight pyramid. In the first scheme, the monument had the same structure as a multi-story building, each floor getting smaller to reduce the loads as it was growing taller. The second scheme was a first attempt to build a straight pyramid but the initial angle was too steep, which was realized in the middle of construction and changed. Finally, after reviewing calculations, Egyptians were able to come up with straight pyramids. In all three cases, masonry (bricks) was used, thus increasing the weight of the structure, and loads needed to be mainly transferred in a vertical way directly to the ground. A pyramid like shape allows the center of gravity to be lower to the ground, therefore reducing the challenges faced by slender buildings.

1.1.2.2 Greek and Roman Temples

These buildings were mostly built in countries around the Mediterranean Sea and were used as places of worship. However, they were structurally very poor, as they were mainly using stones (very efficient in compression, but poor in tension) for all of their members, even beams, which have tension in the bottom. As can be seen in Figure 1.3, the drawback of that was that they had to use a fair amount of columns in order to shorten the spans between columns. Nowadays, the fact that most temples are in ruins is one of the indicators that choice of material and good analysis of structure is extremely important in the conservation of a building.

Figure 1.3: Ruins of Parthenon [4]

1.1.2.3 Cathedrals

Built in the middle ages, these structures were used for Christian churches across Europe. Not only were they a symbol of the Church's power and of the people's respect to God, they were also built high as a means of positioning and locating oneself. Like pyramid and temples, cathedrals were mainly built with masonry, and are not as slender as current buildings. However, because so many were built over such a long period, many schemes were developed throughout the years in order to find ways to transfer loads, namely arch, domes and buttresses for example. These solutions were developed over time by architects and engineers as cathedrals reached increasing heights.

1.1.2.4 Pagodas

Mainly found in Middle-Eastern and Asian countries, they were a lot less high than pyramids, but were very slender, making them structurally more challenging, and more comparable to today's modern high rise buildings. In Japan, some pagodas have been known to withstand earthquakes for more than 1300 years, and make them very interesting structurally.

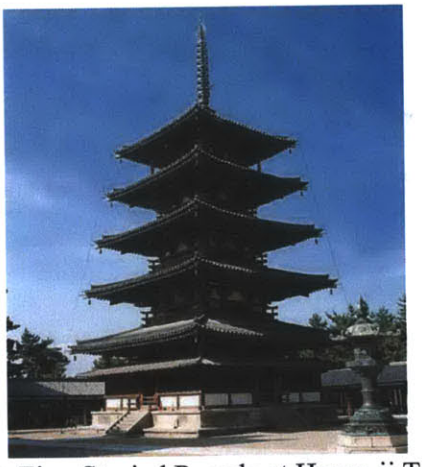

Figure 1.4: Five-Storied Pagoda at Horyu-ji Temple [5]

Because they are confronted with so many earthquakes, Japanese have always been very knowledgeable in structural engineering. Structures of pagodas are a very good example of that

knowledge. The reasons why some of the oldest pagodas still stand nowadays after so many earthquakes can be explained through 5 different structural features [5]:

- Pagodas are made of wood, a very flexible material which can bend without breaking, unlike masonry which makes the building very stiff.
- Connections used in Japanese pagodas are mortise joints, which induce a lot of friction between members, dissipating the energy at the base of the tower.
- The connections between each floor allow them to move independently from one another.
- The shape of the different floors (upside-down bowl) makes each floor move in a different direction, keeping the overall building in place – if the first floor moves to the right, the second floor will slip to the left, making the third one moving toward the right etc.
- Pagodas also have a central pillar (called *shinbashira*) that goes all the way through the pagoda. Much like the concrete cores in modern high-rise buildings, this structural feature allows the structure to remain still, and in this particular case, to hold the different floors together.

Apart from pagodas, which are more specific, tall buildings in the past were mainly built using masonry. Hence, they were very heavy, and the only way of building high, was to build large as well, in order to keep the slenderness of the building fairly low. In this sense, old buildings were facing different challenges from today's modern building (more slender) which are now closer to cantilever bending beams. Although old buildings were working as shear beams, they still had to face challenges when trying to build upwards, and engineering ideas and features were developed as height was increased. Although those ideas are sometimes very innovative, they cannot be used in modern buildings, because we are nowadays constrained to build on smaller areas, hence have more slender designs.

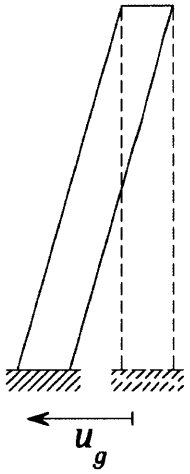

Figure 1.5: Effect of Ground Motion in Flexible Buildings – The Top Remains Still

However, most structural features used in Japanese pagodas are still used nowadays in tall buildings. First of all, tall buildings are more flexible structures, which makes them less vulnerable to earthquakes (See Figure 1.5), but more vulnerable to wind. Second, energy dissipation is a very important issue, which can be achieved through deformation of material or friction like in the pagodas, but which is attained nowadays with the use of dampers (although some friction dampers are known to be used). Third, the use of central pillar is widely used in modern buildings: they are now called cores and are almost always made of concrete.

Unfortunately the use of the individual floors moving independently is a scheme that cannot be used in current buildings. Indeed, this solution, although viable in the long term because the structure stays in place, cannot be implemented in modern use, because it allows the building to move too much when a force is applied. Today, we mainly focus on the everyday comfort of the user rather than the long term stability structure of the building, as will be discussed in section 2.1.2.

1.2 From Past to Present

The pyramid of Cheops (believed to be between 137 and 139m high ~ roughly 450 to 455 feet) was the highest building for about 3750 years, when it was first surpassed in 1220 by Notre Dame the

Rouen (151m ~ 495 feet), and later by only three other cathedrals (Notre Dame de Strasbourg built in 1439, St. Nikolai built in 1874 and Kölner Dom built in 1880)[2]. These cathedrals were then surpassed by the Washington Monument in 1884, an obelisk in Washington D.C. which culminates at 555 feet 5⅛ inches. The Washington Monument is much more unique in the fact that it was one of the first and tallest structures with such slenderness (55 feet square base; roughly a slenderness ratio of 1/10).

However, at that time, only monuments and unique buildings could reach such a height, and tall buildings were not considered an option for more common usage (such as habitation or workplace), mainly because of several problems resulting from those heights.

Figure 1.6: Washington Monument, Washington D.C. [6]

First of all, people would have to walk an important amount of stairs to reach the higher floors. Second, the use of masonry made the development of high rise buildings very impractical, as the higher buildings were, the heavier they were, and the thicker basement walls had to be. To give a rough estimate, in the early 19th century, buildings never went higher than 6 to 10 stories high.

This all changed with the invention of the safety elevator by Elisha Otis in 1852, which took care of the inconvenience caused by too many stairs. Unlike primitive elevators that had already existed for centuries, this new safe elevator provided a way to stop the elevator even if a cable would

break, making it safely usable by the general public. Around the same time, in the late 1850's, modern steel industry started developing, thus introducing a whole new approach in building design. Instead of using heavy masonry, engineers started using light frames which solved the problem of thick walls. The Eiffel Tower designed by Gustave Eiffel and built in 1889 for Paris' World Exposition, was the tallest steel structure at that time. With a roof height of 300m (986 feet), the Eiffel Tower – Figure 1.7 - symbolizes the new era brought by steel in building engineering, and initiated the race for high-rise buildings.

With those two inventions, development of high-rise buildings as we know them could start. The first steel-frame tall buildings were mostly built in Chicago, New York and London. Early skyscrapers were generally in the order of 15 to 30 stories high. The Eiffel Tower remained the tallest structure or 41 years, when surpassed by the Chrysler building in 1930 and later by the Empire State Building in 1931, which were the first skyscrapers as we now know them.

Figure 1.7: Eiffel Tower, Paris [7]

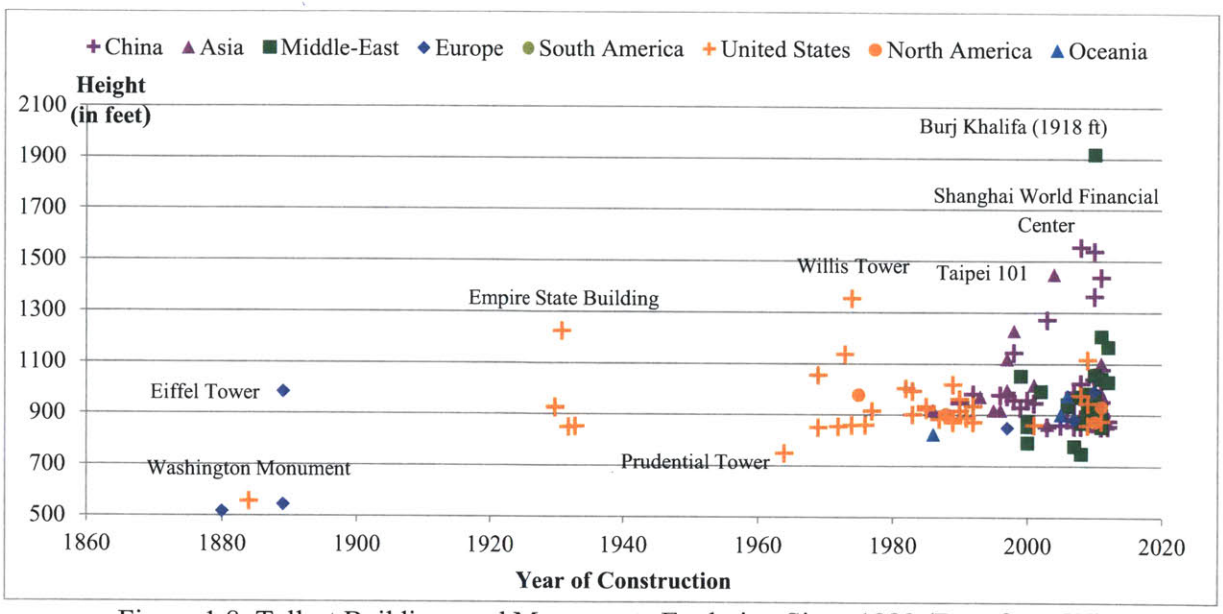

Figure 1.8: Tallest Buildings and Monuments Evolution Since 1880 (Data from [2])

Figure 1.8 shows the evolution of buildings higher than 850 feet since 1880, in comparison to Washington Monument, the Eiffel Tower, and two other Cathedrals in Europe. Prudential Tower is also introduced as a reference point for MIT Students. The chart gives the height of the highest floor of the buildings – data gathered from SkyscraperPage.com [2] - which is not necessarily the same as the official height of a building (See section 1.3 for more details).

1.3 High-Rise Buildings Today

Nowadays, most reasons why we try to build taller and taller structures are different from the past:

First of all, with a constantly growing population, it has become crucial for cities to grow taller rather than expand larger, namely to reduce travel distances inside a city. In specific cases, cities are constrained by their available building area, like in Chicago during the 1870's, when the expansion going on was so important that the city soon reached its natural boundaries [8]. Because of that, the only way to increase capacity of the city was to build up.

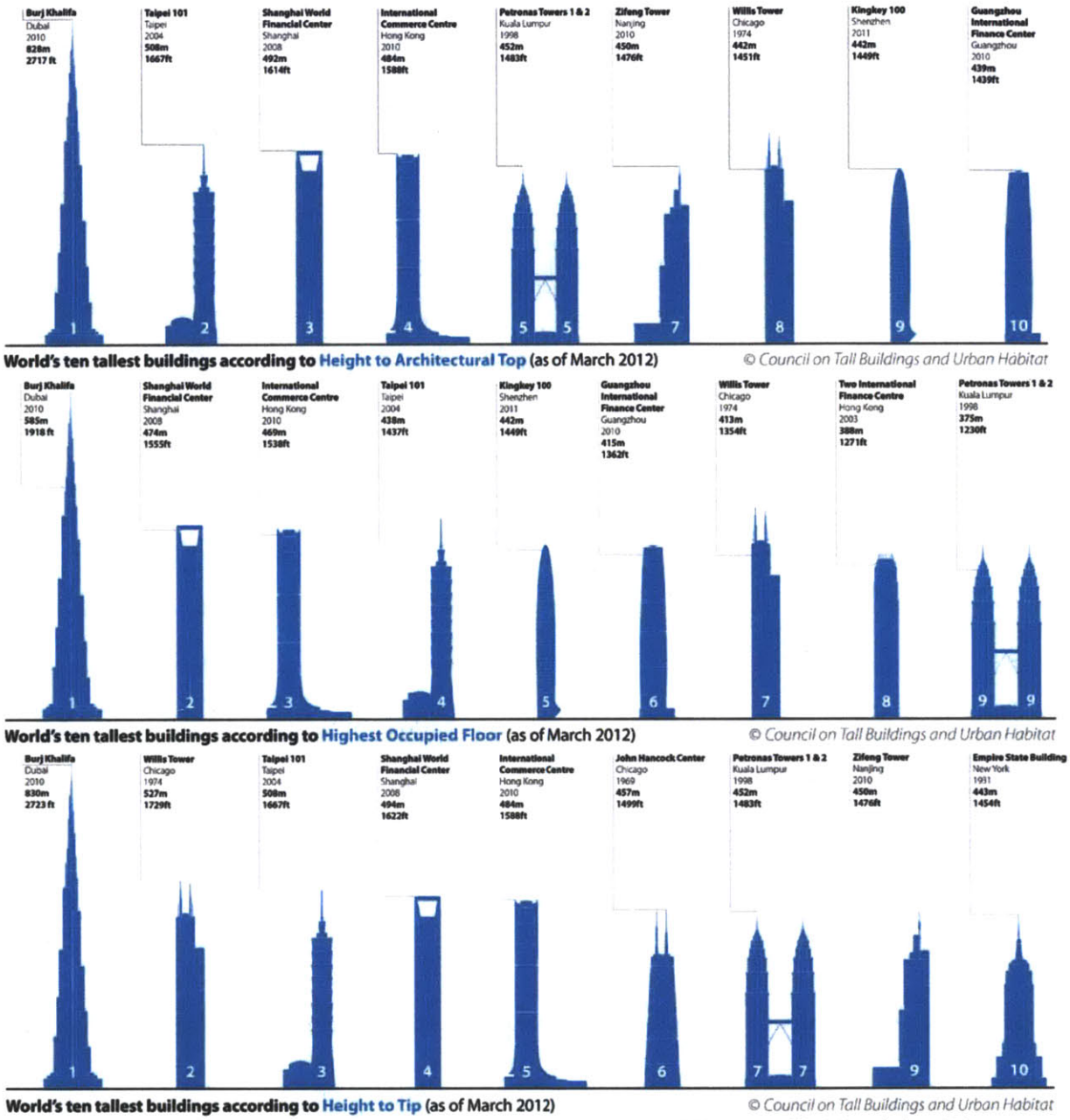

Figure 1.9: Ten Tallest Buildings According to Three Different Official Heights [9]

Building high-rise buildings is still a mean of showing wealth and technological advance, as it was in the past. Because of that, people have defined several heights for a building, allowing skyscrapers to be taller when considering a specific height, and shorter when considering another height. The different heights include: height of the highest occupied floor, height of the highest architectural feature (spire), or height of the highest tip (including functional feature such as communication antenna for example). Figure 1.9 shows the impact of such definition when ordering

buildings according to their heights. Most of the time, architectural height (spire) will be considered to be the official height of a skyscraper.

This paper focuses mainly on ways to mitigate motion for human comfort. Because of that, Figure 1.8, Figure 1.10 and Figure 1.11 are based on the height of the highest occupied floor (when known) – data provided by SkyscraperPage.com [2] and by The Council on Tall Buildings and Urban Habitat (CTBUH) [9]. Therefore, some discrepancies can be found with official heights of building.

Building high is also sometimes viewed as a competition between countries, or even simple owners, architects or builders. It can be seen through Figure 1.10 and Figure 1.11 that Skyscrapers are a good indicator of a country's economy (see section 1.3.1 for more details). A good example of this desire to build the tallest structure in the world is the tower Taipei 101, built in 2004 in Taipei, Taiwan, which was initially designed as a 66 story building, then an 88 story building, to finally reach its current height of 101 stories [10].

1.3.1 List of High Rise Buildings

Figure 1.10 and Figure 1.11 provide a list of the highest skyscrapers since 1930 and since 1982 respectively. Figure 1.11 doesn't show the current tallest building in the world (Burj Khalifa), for ease of reading. What is interesting from those figures is that they reflect the evolution of economy throughout time. The race for the sky started in the early 1930's with Chrysler Building and the Empire State Building in New York. After a short break, partly due to Second World War and the Cold War, the United States started building high in the 1970's related to the economic boom. During the 1980's, it seemed clear that the United States had the technology to build skyscrapers of 1000 feet high without too much difficulty.

It can clearly be seen that China and Asia in general, started building tall structures in the 1990's, as a symbol of their growing economic wealth. Soon, they surpassed the tallest building that had been built so far in the United States, with Petronas Towers (architectural height) and Taipei 101.

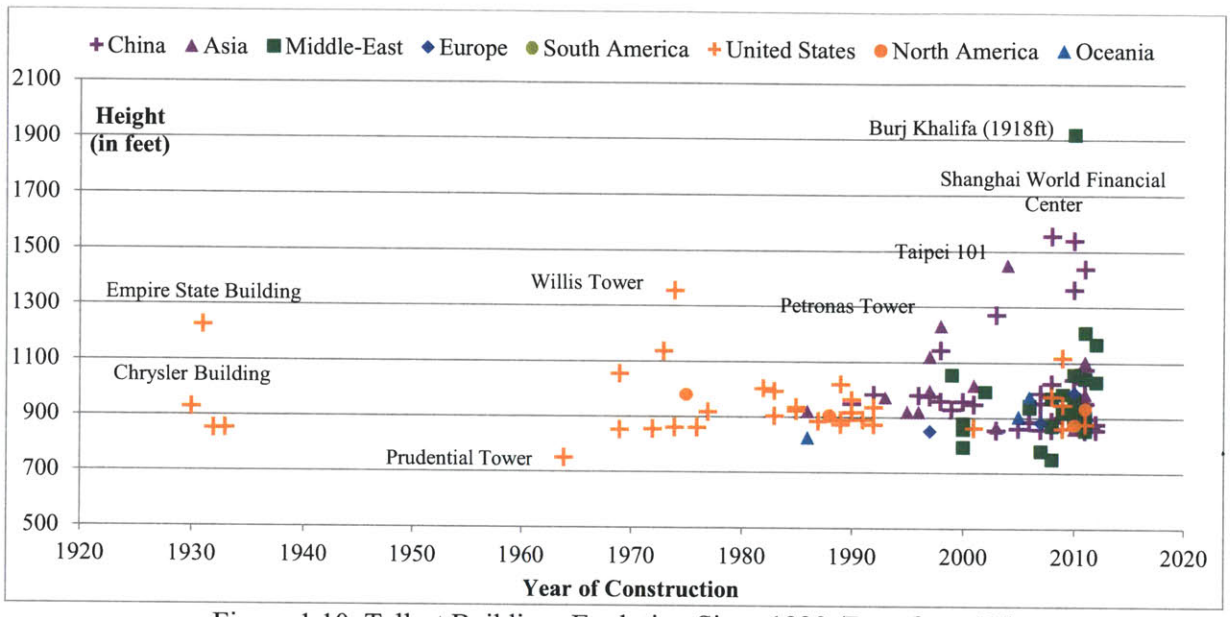

Figure 1.10: Tallest Buildings Evolution Since 1930 (Data from [2])

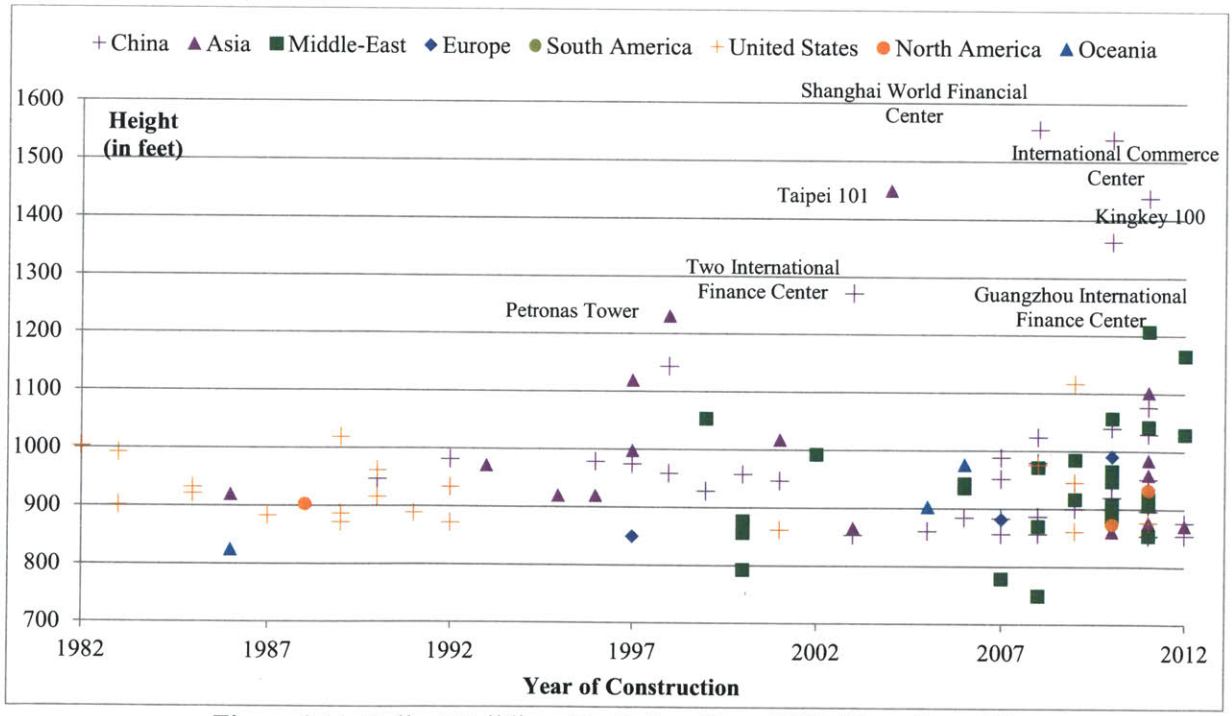

Figure 1.11: Tallest Buildings Evolution Since 1982 (Data from [2])

1.3.2 Examples of Buildings with Tuned Mass Dampers

As will be discussed in this paper – see Chapter 3 - some high rise buildings require auxiliary system known as Tuned Mass Dampers (TMD) in order to cancel the swaying motion due to wind. Below are two examples of buildings with such devices.

1.3.2.1 Taipei 101 [11]

Taipei 101, also formerly known as Taipei World Financial Center, is a 101-story high skyscraper located in Xinyi District, in Taipei, Taiwan (Republic of China), built in 2004. It was the tallest building (architectural height) until 2010, when Burj Khalifa was opened. Currently, it is the second tallest building according to architectural height, and fourth tallest according to highest occupied floor.

A Hybrid pendulum-type Tuned Mass Damper was installed to reduce common winds and typhoons (which are frequent in the area) induced vibrations in the building. The TMD role is mainly to ensure comfort of users, not to provide structural stability. The pendulum consists of steel cables, a mass, a tuning frame, hydraulic viscous dampers and a bumper system. The steel cables hang from the top of the 91st floor down to the 87th floor, and the TMD is open to public view on the 88th and 89th floors. The mass is currently the largest (5.5 meters diameter, made of 41 layers of 12.5 cm thick plates welded together) and the heaviest (660 metric tons) TMD in the world. The building's mass being of 160,000 metric tons, the mass ratio is of 1/242. The tuning frame, located on the 91st floor, supports the cables, monitors building vibrations and adapts the cables' movements to optimize efficiency of the TMD (Although Taipei 101 official website claims the system is passive, it is in fact closer to a Hybrid type of damper, as will be explained in section 3.4.1.3). Eight hydraulic dampers are used to dissipate energy. The bumper system, with 8 additional snubber hydraulic dampers, absorbs vibrations impacts, especially during typhoons.

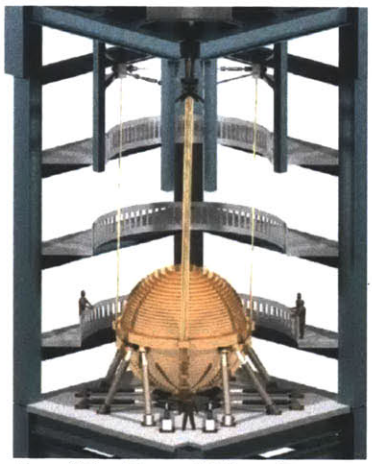

Figure 1.12: Schematic of the Tuned Mass Damper in Taipei 101 [12]

In terms of performance, the TMD has moved up to 35cm during high winds and is designed to be able to move up to 150cm during extreme typhoons (100-year Return Period). It cuts building vibrations by 40%. It was designed, manufactured and constructed by Motioneering Inc. (Canada) for a cost of roughly 4.5 million USD.

In addition to this wind damper, Taipei 101 also uses two smaller dampers (6 metric tons each) on its pinnacle to reduce vibrations by another 40%. Dampers have also been placed on elevators in the building to increase their stability.

1.3.2.2 Shanghai World Financial Center [13]

Shanghai World Financial Center is a 101-story high building, located in the Pudong financial district of Shanghai, China, and built in 2008. It is currently the third tallest building in the world according to architectural height and second tallest according to highest occupied floor.

Two Active Tuned Mass Dampers (first of this type in mainland China) – see section 3.4.1.2 - were installed on the 90th floor of the building. They each weigh 150 tons, and are placed on each side of the building, to prevent swaying due to wind (especially typhoons) in the x direction, y direction, and torsional movement [14]. These AMDs can move in both direction (x and y) and adapt their

movement according to wind loading: sensors can measure movement and wind loadings, and a computer controlled system can then activate the AMDs accordingly.

Chapter 2 - Motion Mitigation in High-Rise Buildings

2.1 New Problems with Taller Structures

With tall buildings comes a whole new approach on design of structure. Indeed, these structures being very flexible, they are more prone to vibrations. Furthermore, their uniqueness might make them react differently to usual loads (wind or earthquakes for example). Therefore, two aspects are to be taken into account:

1) How does loading affect the structure? This will be discussed in section 2.1.1
2) How does vibration affect users? This will be discussed in section 2.1.2

2.1.1 Wind Loads on Tall Buildings [15]

Taller buildings have inherent properties which differentiate them a lot from older, shorter buildings, as will be discussed in the several next sections. Because of that, skyscrapers react differently to wind loads then their older brethren. Not only that, studies show that because of height involved, wind also acts differently on tall buildings than on normal structures. Therefore it is important to study the action of wind and the reaction of structures to those winds in the domain of skyscrapers only.

2.1.1.1 Differences between short and tall structures

The difference between how tall and short building react to wind load can first be explained by the structural differences of these two buildings. Figure 2.1 shows typical dimensions (in meters) of short (traditional) and tall buildings. Dimensions for the short building represent a typical 10-story square building while dimensions for the skyscraper were taken from JinMao Tower in Shanghai, which is 88-story tall.

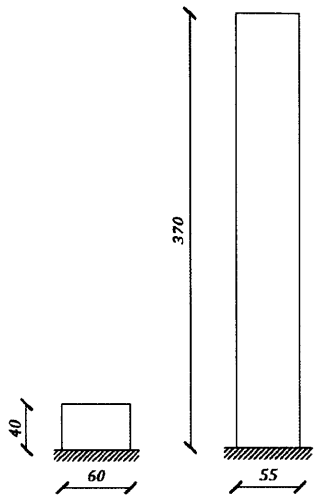

Figure 2.1: Dimensions of Short Buildings versus Dimensions of Tall Buildings (in meters)

As explained in section 1.2, development of high-rise structure was possible with development of new materials (mainly steel) which consequently influenced structure of skyscrapers. In typical shorter buildings, masonry and stone was widely used, both in structural (massive members) or nonstructural (partition walls and façade walls) elements. However in skyscrapers, buildings became roughly 8 to 10 times taller, while keeping the same (or sometimes smaller) footprint area. In order to not drastically increase foundations capacity, construction evolved to much lighter buildings, using lightweight curtain walls, dry partition walls and high-strength material. However, by reducing mass distribution of the building, tall buildings also lost the high-damping and high-stiffness advantages of heavy material.

2.1.1.2 Wind Frequency (Along wind)

When considering wind velocity, it can be modeled very simply as a sum of a constant flow and a dynamic component [16], as expressed in (2.1), where $\overline{V}(z)$ is the *mean wind velocity* (constant flow), and $u(z,t)$ is a random *gust-effect* (dynamic component).

$$V(z,t) = \overline{V}(z) + u(z,t) \tag{2.1}$$

This can be felt during windy days, when one can feel a constant steady flow of wind, while randomly experiencing sudden gusts of rushing winds. Little study has been led in terms of wind gust effects, mainly because they have not yet proven to cause major structural damage. However during heavy windstorms they can cause motion sickness – see section 2.1.2 – or nonstructural damage (vibrating objects, swinging doors, falling books, or in worst case scenarios, breaking glass which causes safety issues for exterior pedestrians). A rough estimate of gust-effect speed can be taken to be 30% of mean speed and direction of gust can deviate up to 30 degrees of the mean velocity direction [17].

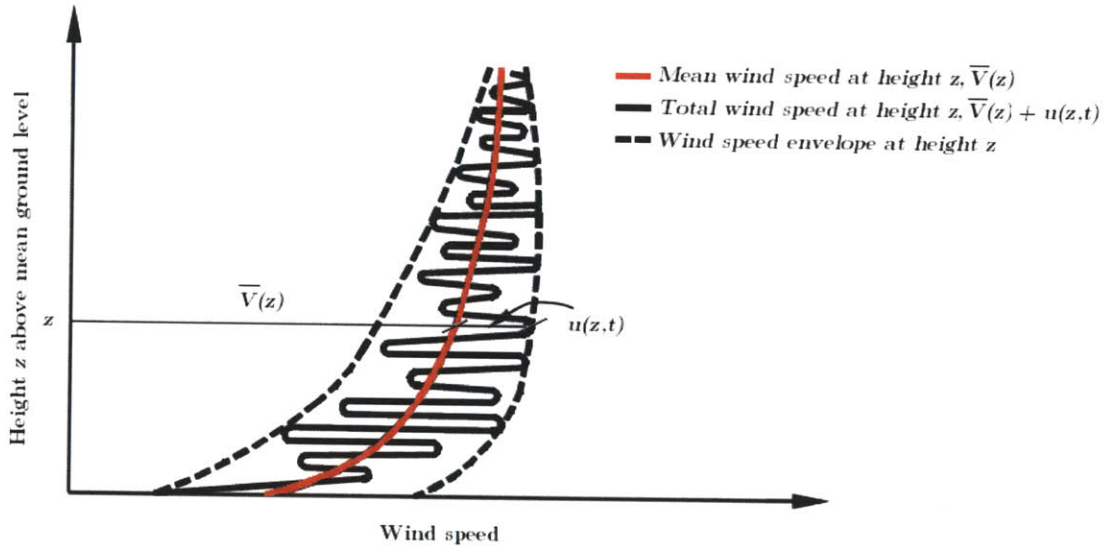

Figure 2.2: Wind Speed According to Height, at Fixed Time t (Adapted from [15])

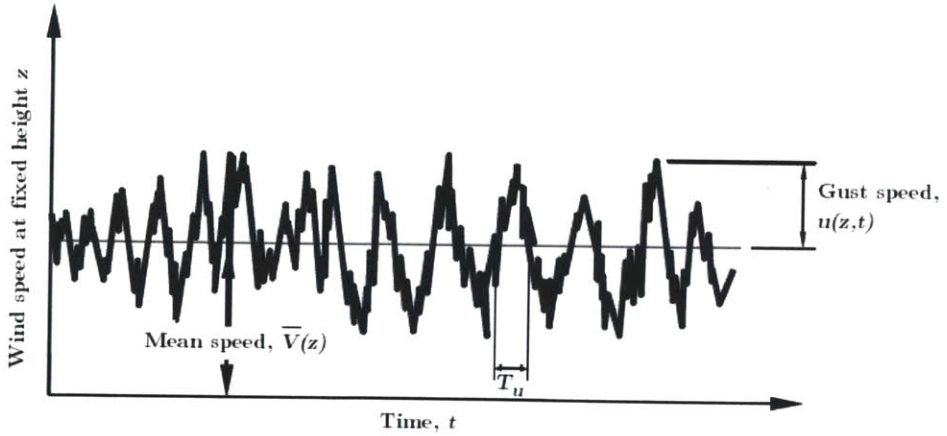

Figure 2.3: Wind Speed According to Time, at Fixed Height z (Adapted from [15])

The gust-effect varies according to height (see Figure 2.2) and time (see Figure 2.3). Because of those variations, gust effects must sometimes be considered as dynamic loads, according to properties of the building.

2.1.1.2.1 Natural Frequency of Building

A general rule of thumb states that the period of a building (in seconds) is roughly equal to N/10, where N is the building's number of stories.

As an order of magnitude of the period of tall buildings, the Chrysler Building - which can be considered one of the first skyscrapers - is 77 stories high. Its natural period is roughly of 7.7s which corresponds to a natural frequency of 0.13 Hz. On the other hand, Taipei 101, the second tallest building, is 101 stories high, with an approximate natural frequency of 0.09 Hz. This gives a rough estimate of current skyscrapers' frequency to be around .09 to .15 Hz i.e. a natural period around 7 to 10s.

Short buildings – 5 to 10 stories – have a natural period of 0.5 to 1s, corresponding to a natural frequency of 1 to 2 Hz.

2.1.1.2.2 Effect of Wind Gust

Although wind load cannot be considered as a period excitation, it is possible to find a pseudo-period of wind-gust, named T_u in Figure 2.3, which is usually in the order of 2 to 3s. When comparing the T_u period to the natural period of buildings, we get

$$T_{short\ buildings} \ll T_u \ll T_{tall\ buildings}$$

Therefore, gust effects seem much longer for short buildings, and can be considered to be quasi-static loads. However, for tall buildings, this assumption is not true anymore and dynamic loads must be considered. Although this dynamic effect is mainly considered on the structure, it can in certain case directly affect nonstructural elements (such as cladding or window glass).

2.1.1.3 Velocity Profile

When considering mean wind velocity only, speed increases with height, mainly because when close to surface, friction is caused with the ground and a drag effect can be seen, reducing low height speed. The drag effect depends on the roughness of the ground, which varies with location. For this reason, the American Society of Civil Engineers (ASCE) defined 4 types of *Exposures* – Exposure A (meant for heavily built-up city centers) was then removed in the 2002 edition of ASCE 7.

Once a certain height – called the *gradient height* – is reached, the drag effect becomes negligible, and wind speed is considered to reach a maximum value – called the *gradient velocity*. The height for which wind is affected by topography – between ground level and the gradient height – is called the *atmospheric boundary layer*, and only in that layer does the mean wind speed profile varies, according to equation (2.2) and values from Table 2.1. Past the boundary layer, mean wind speed is considered constant.

$$\overline{V}(z) = V_g \left(\frac{z}{z_g}\right)^{\frac{1}{\alpha}} \tag{2.2}$$

Where

$\overline{V}(z)$ is the mean wind speed at height z above ground
V_g is the gradient wind speed assumed constant above the boundary layer
z is the height above ground
z_g is the gradient height (or height of the boundary layer)
α is the power law coefficient

Exposure / Terrain type	α	Gradient height z_g	
		(m)	(ft)
A, Urban (*)	5	457	1500
B, Suburban	7	366	1200
C, Open Country	9.5	274	900
D, Very Smooth	11.5	218	700

(*) Exposure A has been removed, and urban terrain are now considered part of Exposure B

Table 2.1: Values for the Power Law Coefficient [18]

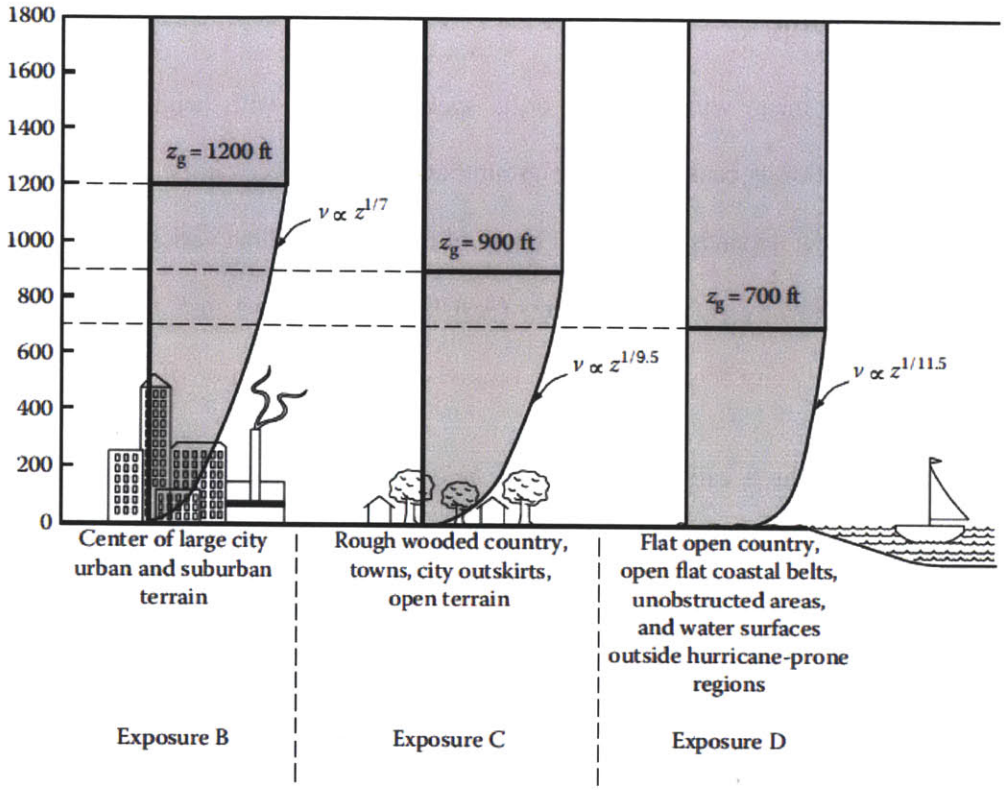

Figure 2.4: Velocity Profile of Mean Wind According to Exposure [15]

Figure 2.4 shows the velocity profile of mean wind, according to exposure. As expected from equation (2.2) and values from Table 2.1, gradient wind speed is attained faster when there is less drag effect. This mainly shows that wind speed is more important at the top of skyscraper, which consequently increases the risk of vortex shedding effect (see section 2.1.1.4)

2.1.1.4 Vortex Shedding (Transverse Wind)

Another phenomenon which occurs with tall slender buildings and wasn't considered in buildings before the race towards the sky is the vortex shedding effect (although this effect had already been seen with slender structures, such as chimneys or lampposts). Wind produces not only an along wind force – which was the force discussed in sections 2.1.1.2 and 2.1.1.3 – but also a transverse wind force, perpendicular to the main flow of wind. This is illustrated in Figure 2.5, which is a simplification of what is happening in reality. Indeed, in a 3D model, wind also goes above the

structure, having the exact effect along the vertical axis. However, these effects (called *lift* and *yawn* effects) are negligible compared to the transvers force effect.

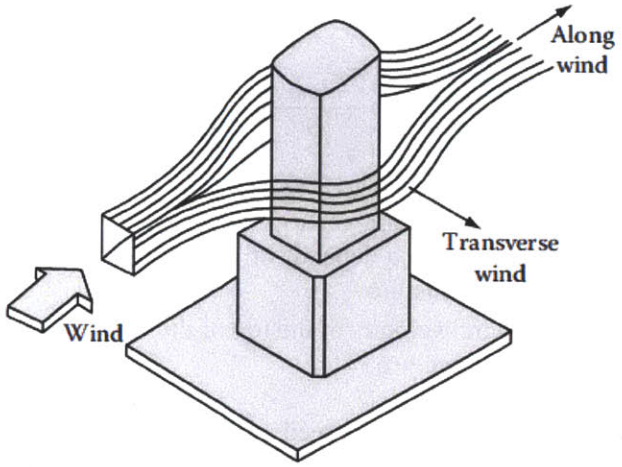

Figure 2.5: Simplified 2D Wind Flow Showing Along and Transverse Effects [15]

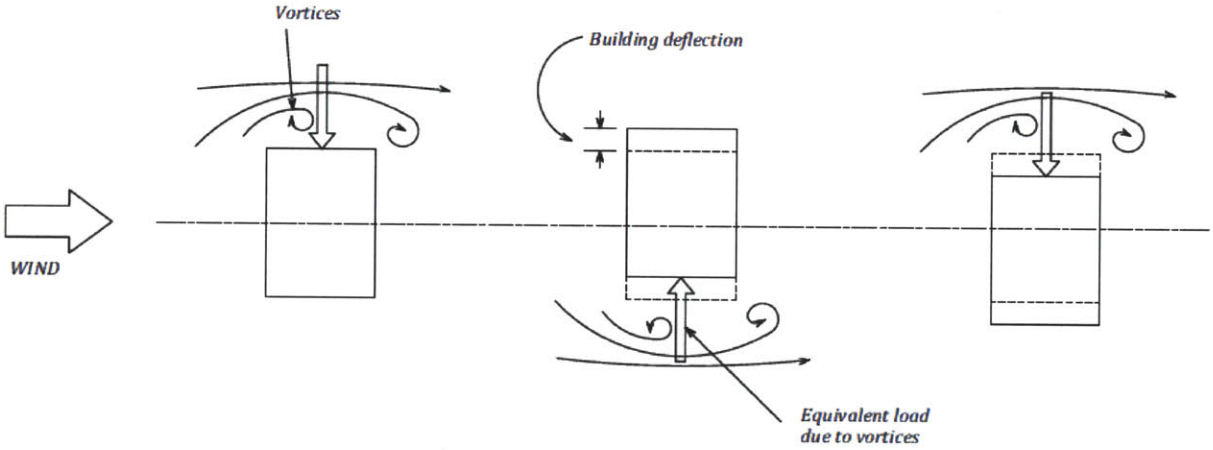

Figure 2.6: Periodic Shedding of Vortices and Response of Building (Adapted from [19])

When wind hits a slender structure, it flows along its side, while air stays in contact with the surface of the structure's sides. However, if the wind facing side of the building is too sharply convex, or if the wind speed is too high, air will leave the side of the structure. This will create a zone of negative pressure, where vortices and eddies will form [19]. This will push the structure on one side, initializing a swaying motion of the building. As the building sways, it will impact on the flow of wind: when the building moves towards the left, more wind will flow towards the right, creating another transverse force, increasing the swaying effect, etc. This effect, which occurs more frequently at high wind speed, is illustrated in Figure 2.6.

Because of the periodic characteristic of vortex shedding, transverse wind effect has, in general, a much more severe effect on structures. The periodicity is determined by the Strouhal number through the following equation:

$$f = S \frac{\overline{V}(z_{max})}{D} \tag{2.3}$$

Where

f is the frequency of the shedding vortices in Hz
S is the *Strouhal number*, which depends on the geometry and wind speed
z_{max} is the height of the structure
$\overline{V}(z_{max})$ is the mean wind velocity at the top of the structure
D is the diameter of the structure

The Strouhal number increases with wind speed, and varies with the shape and surface of the structure. As an example, for a smooth cylindrical structure, the Strouhal number increases from 0 to 0.20 for winds going from 0 to 50mph (22.4m/s). It then almost stays constant for winds going up to 150mph (51m/s), although it can still increase up to 0.21 for winds faster than 150mph. Therefore, the Strouhal number is usually estimated at 0.20, although for exact values, wind tunnel testing is required.

If the frequency of the vortex shedding effect reaches the natural frequency of the building, harmonic excitation occurs. This is reached whenever the mean wind speed reaches the values given by equation (2.4), which combines equation (2.3) with the rule of thumb from section 2.1.1.2.1, where n is the number of stories of the building. A rough estimate for the JinMao tower (60m diameter, 88 stories high) would be a speed of 34m.s^{-1}, which is easily attainable.

$$\overline{V}(z_{max}) = f \frac{D}{S} = \frac{10}{n} \frac{D}{S} \tag{2.4}$$

Once harmonic excitation occurs, a *Lock-in* phenomenon occurs, where the building stays in harmonic excitation even if the wind speed slightly changes. The lock-in phenomenon keeps happening roughly at ± 10% of the building's natural frequency.

Type	Short (Usual Building)		Tall (Skyscrapers)	
Mass	Heavy	due to heavy masonry	Light	due to light-weight materials
Damping	High		Low	
Period	0.5 to 1s		7 to 10s	
Gust period	2 to 3s			
Gust effect	Static loading		Dynamic loading	
Risks	- None		- Motion sickness - Nonstructural damage - Harmonic excitation (rare)	
Wind speed	Low		High	
Others	- None		- Vortex shedding risk	

Table 2.2: Wind Effects on Short and Tall Buildings

Table 2.2 gives a summary on the effects of wind on tall buildings, in opposition to traditional buildings. Although some risk for structural damage exists, in most cases the nonstructural damages are worst, especially motion sickness, which will be discussed in the next section.

2.1.2 Motion Sickness [20]

2.1.2.1 Extrapolation

Before 1967, very little research had been led in terms of motion sickness in building. Data was first collected in an attempt to correlate movement and motion sickness in ships. McCauley and O'Hanlon's model (1976) [21] can be seen in Figure 2.7. It shows the correlation between Motion Sickness Incidence, Frequency, and Root Mean Square (RMS) Acceleration. However, the model had limitations in the sense that it only referred to seasickness: it has been noticed that motion sickness in ships is primarily due to vertical acceleration, and occurs only after 2 to 3 days of continuous excitation.

Using the rule of thumb given in section 2.1.1.2.1, a rough estimate of current skyscrapers' frequency is of 0.09 to 0.15 Hz. Considering the fact that ships have a frequency between .1Hz and .3Hz [20], data for ships can be used as a first approximation for tall buildings.

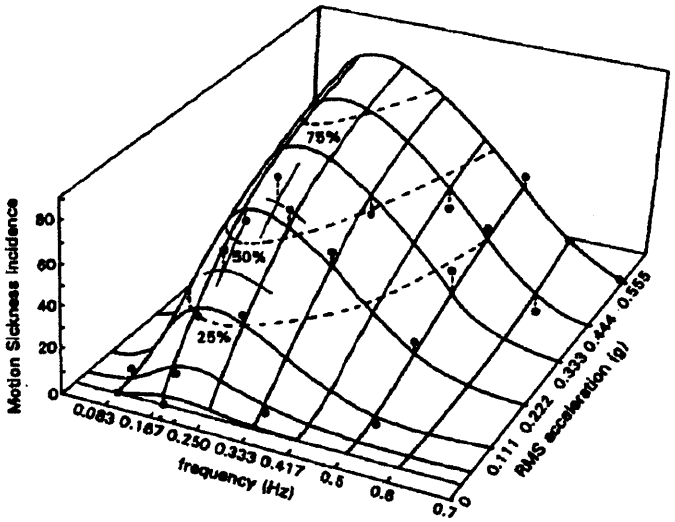

Figure 2.7: McCauley et al (1976)'s Motion Sickness Model [21]

Chang was one of the first (1967) to come up with the idea of seeing the human comfort criteria as a limiting constraint in building design. One of the consequences of his study was his suggestion to reduce the considered Return Period: the typical 50 years Return Period had to be shortened to 10 or even 2 years. He used data collected from experiments of comfort at high frequency to extrapolate a low frequency comfort graph. This can be seen in Figure 2.8.

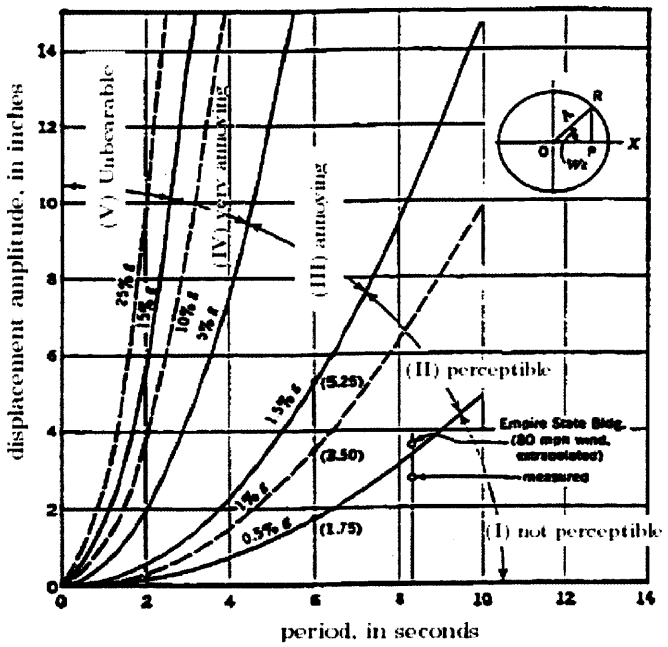

Figure 2.8: Comfort Criteria According to Frequency and Amplitude [22]

2.1.2.2 Physical Simulation – Moving Rooms

In 1972, Chen and Robertson [23] were the first to physically experiment on low frequency excitations effect on motion sickness – unlike the previous extrapolation methods used at the time. Their experiment consisted of a small room (2.74m by 4.88m with a height of 2.67m) without any windows (to remove visual cues) on wheels, which was excited horizontally. People were asked to go inside the room and their reaction was measured with regards to specific criteria: their expectation of motion (a), their posture and movement (b), their orientation (c), and the frequency of the excitation (d).

(a) Three cases were considered. In the first case, people didn't know the room would shake. In the second case, they were told the room would shake. In the third, they had already experienced the shaking and were asked to go in the room a second time.

(b) Three positions were considered: sitting, standing still, or walking.

(c) Orientation parallel and perpendicular to movement were considered. They did not seem to affect motion sickness a lot.

(d) The room was excited with three different frequencies: .067Hz, .1Hz and .2Hz (Close to previous estimate of periods in skyscrapers). These are the respective frequencies for 5s, 10s and 15s periodic excitations.

Several conclusions came out of this experiment regarding the thresholds of motion perception, and apart from orientation, all the other factors play an important role in motion detection:

- Expectation of motion lowers the perception threshold.
- Standing still lowers the threshold (in contrast to sitting or walking).
- Threshold increases as the frequency decreases (from .2 to .067Hz).

2.1.2.3 Survey on Actual Buildings

In 1973, Hansen, Reed and Vanmarcke took the experimentation to another, more realistic level [24]. In 1971, during passing of a winter storm, users reported perception of motion in two separate buildings. These buildings were in two separate cities, both 550 feet high (roughly), and office buildings. The storms lasted respectively 5 and 6 hours, with a peak motion of respectively 30 and 20 minutes. A survey was then conducted by the authors to understand how many people felt the motion, and out of those who did feel it, what cues led them to feel it, and how tolerable it was.

Motion Cue	Building 1			Building 2		
	% who noticed	1st most noticeable (%)	2nd most noticeable (%)	% who noticed	1st most noticeable (%)	2nd most noticeable (%)
Movement of doors, fixtures, etc.	56.2	18.8	9.4	64.1	9.4	37.7
Creaking sounds	92.1	28.1	34.4	64.1	20.8	26.4
Feeling self-movement	62.5	28.1	17.2	69.9	51	15.1
Looking out window	62.5	4.7	10.9	11.3	1.9	3.8
Comments from co-workers	37.5	12.5	7.8	17	11.3	-
Other [1]	46.9	4.7	12.5	34	-	1.9
No preference	-	3.1	7.8	-	5.6	15.1
Not knowing building was moving	-	-	-	5.6	-	-
Total		100	100		100	100

[1]Other includes elevator noise, wind whistling etc.

Table 2.3: Noticeability of Motion Cues [24]

Table 2.3 [24], summarizes the list of cues that led people to feel the motion. Interviewees were asked to give the cues on their own, and after that, were asked about the other cues. It is interesting to look at the "look out the window" cue. Indeed, this should be noticeable only in torsional movement, and although building 1 was more flexible in this direction, it is strange to see that so many people (62.5%) said they noticed this cue. On the other hand, it shouldn't have been noticeable in building 2, which was much stiffer in torsional movement, yet some people (11.3%) noticed it. It

might be possible that other cues led people to feel movement, and probably made them imagine seeing visual cue by the window, however 70% of interviewees correctly identified the period of peak motion (within a one hour range), leading to believe they had accurate perception of motion.

The authors then focused on how tolerable this motion was. They asked interviewees if they would object to such motion, given different rates of occurrence of the storms (The "no objection ever" category was included only after indicated by a considerable number of interviewees). It is important to notice the authors were looking for tolerance levels, and not perception levels, unlike what had previously been done. Results are summarized in Table 2.4.

% of people who would object if storms occurred	Building 1	Building 2
No objection ever	21.8	27.9
Once a day	68.8	46.5
2 – 5 times a year	7.8	14
Once a year	1.6	11.6
Once every 5 years	-	-
Total	100	100

Table 2.4: Percentage of Objections versus Occurrence Rate [24]

The study ended with a suggested recommendation for building design, after having asked several engineers as well as building owners. Engineers mostly feel that it would be unacceptable for more than 2% of the users to feel motion, and owners tend to agree that over the same 2%, the project would become non-profitable. Thus the design criterion recommended by this study was to allow no more than 2% occupant objection for a 1 year Return Period wind.

2.1.2.4 Recent Studies

Further studies have since been led to try and get more accurate results, although they are still based on the same principles (moving rooms and surveying real buildings). The idea was to overcome several limitations of previous studies such as:

- Get a more accurate representation of excitation in moving rooms. Primitive experiments only tested straight sinusoidal excitations, which is not necessarily a truthful representation of reality.
- Try to include visual and auditory cues in moving rooms, which seemed to play a significant role in motion tolerance [24].
- Take into account the fact that each individual has a different sense of perception.
- Acquire more data in high-rise buildings so as to validate lab results. This was recommended by the CTBUH [25], which is an international not-for-profit organization focusing on sharing information on tall buildings and founded in 1969.
- Give more importance to the location (height/floor) of the interviewees during excitation in real case studies.

The most interesting conclusions that came out of those more recent studies are summarized in this section. The first result is related to wind tunnel testing. Isyumov and Halvorson [26] compared measurements for a monitored 71-story building with prevision from wind tunnel testing. The results, which confirm the accuracy of wind tunnel testing, can be seen in Figure 2.9.

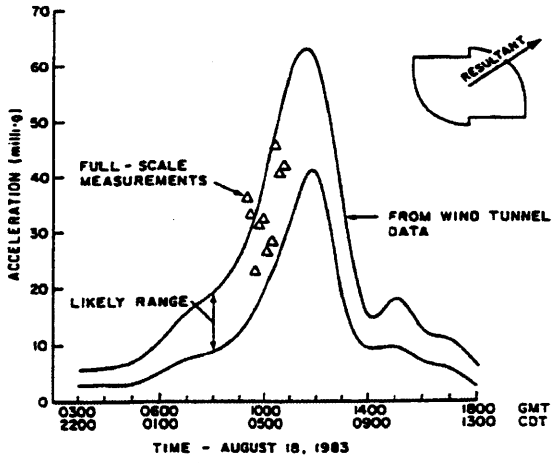

Figure 2.9: Peak Resultant Acceleration at 71st Floor during Alicia Compared with Predicted Wind-Tunnel Testing Results

Another interesting result is related to difference in perception according to people. Kanda, Tamura, Fujii, Ohtsuki, Shioya and Nakata [27] led moving rooms experiments in 1994 to see the

effects on random motion in opposition to sinusoidal motion. It turns out the difference weren't significant. Results are shown in Figure 2.10.

Another study [28] led in 2006, showed that elliptical motion didn't have a significant influence on the perception thresholds of people, as can be seen in Figure 2.11. The different excitations are: (a) fore and aft, uniaxial X, (b) side to side, uniaxial Y (c) fore and aft, elliptical X, (d) side to side, elliptical Y, (e) circular. Subjects were seating and facing the fore and aft (X) direction.

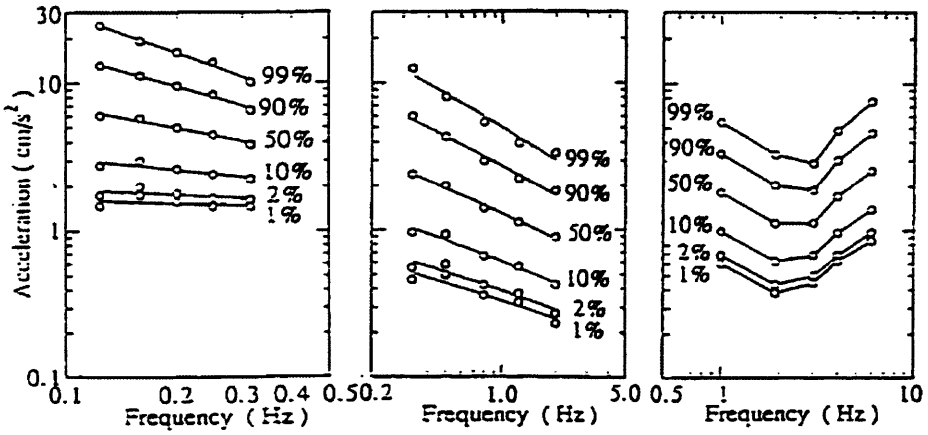

(a)Low frequency set (b)Middle frequency set (c)High frequency set

Figure 2.10: Probabilistic Perception Thresholds for Uni-axial Sinusoidal Motion [27]

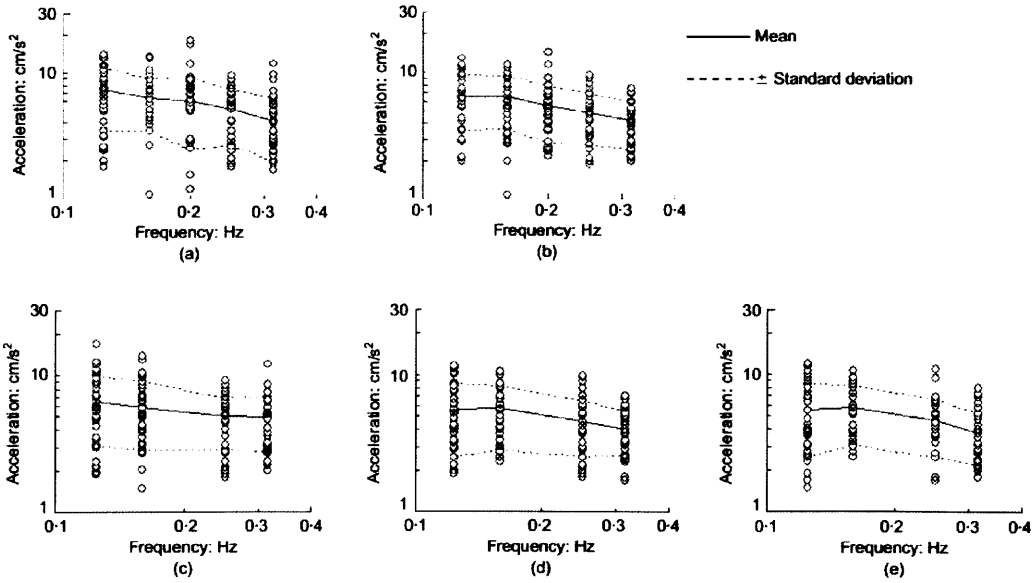

Figure 2.11: Perception Thresholds by Individual Subjects for Low Frequency Set [28]

According to Figure 2.10, results for the recommended 2% probability [24] at low frequency do not depend very much on the frequency. Because those frequencies are the most likely to create discomfort, Isyumov had the idea to give criteria according to allowable peak resultant acceleration and torsional velocity at top floor [29]. Indeed, these movements are the ones who create visual cues, which in turn create discomfort. His guidelines are shown in Table 2.5.

Both requirement 1 and 2 should be satisfied		Acceptable hourly peak values	
		Once per year event	Once per 10 year event
1) Peak resultant accelerations at the top floor should be at or below	Residential	0.005 – 0.007g	0.010 – 0.015g
	Hotels	0.007 – 0.009g	0.015 – 0.020g
	Office	0.009 – 0.012g	0.020 – 0.025g
2) Peak torsional velocity at top floor should be at or below	All occupancies	0.0015 rad/sec	0.0030 rad/sec

Table 2.5: Tentative Guidelines for Evaluating the Acceptability of Wind-Induced Motions of Tall Buildings [29]

2.2 Motion Based Design [30]

Traditional structure design is based on a strength based approach: engineers designed structures and buildings with the requirement for them not to fail, and later checking whether requirements for serviceability were met. However, in the case of skyscrapers, structures have drastically changed, and although strength is now less of an issue when building high, motion has become one of the key problems to solve when designing a tall building, as discussed in the previous section. Therefore a new approach has been developed, where engineers first try to solve the motion issues, which most of the time complies with the strength issues.

As a quick example, a first approximation model of a skyscraper can be a simple cantilever beam, as shown in Figure 2.12. Two approaches can be taken to size the beam, i.e. find the appropriate moment of inertia.

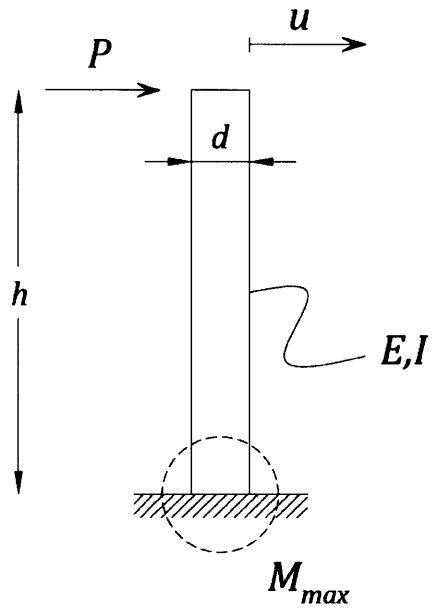

Figure 2.12: Simple Cantilever Beam Model of a Tall Building

Strength Based Approach: in this approach, the constraint is given by a maximum allowable stress in the material. The maximum stress in the beam is given by the equation

$$\sigma_{max} = \frac{M_{max} d}{2I} \leq \sigma^* \tag{2.5}$$

Where

σ_{max} is the maximum stress in the beam (located at the base)
$M_{max} = Ph$ is the maximum moment in the beam (located at the base)
d is the width of the beam
I is the moment of inertia
σ^* is the maximum allowable stress in the material

In this approach, the minimum required moment of inertia of the beam is

$$I_{strength\ based} = \frac{Phd}{2\sigma^*} \tag{2.6}$$

Motion Based Approach: in this approach the constraint is given by a maximum allowable deflection at the top of the building. In building codes, this deflection is usually a function of the height of the structure ($u \leq \frac{h}{\alpha}$). The maximum deflection in the beam (at the top) is given by the equation

$$u = \frac{Ph^3}{3EI} \leq \frac{h}{\alpha} \tag{2.7}$$

Where

u is the maximum deflection of the beam (located at the top)
E is the Young's Modulus of the material
h is the height of the beam
α is a value given in building codes and varies from 300 to 500.

In this approach, the minimum required moment of inertia of the beam is

$$I_{motion\ based} = \frac{P\alpha h^2}{3E} \tag{2.8}$$

The moment of inertia picked when designing the beam should satisfy both strength design and motion design approaches. However, if we compare both minimum required moments of inertia (from equations (2.6) and (2.8)) in the case of tall building, we get

$$\frac{I_{motion\ based}}{I_{strength\ based}} = \frac{2}{3}\alpha\frac{\sigma^*}{E}\frac{h}{d} \tag{2.9}$$

For illustration purposes, we can pick specific values corresponding to actual capacities:

α = 300
σ^*= 700 MPa
E = 210 GPa
$\frac{h}{d}$ = 7 (slenderness ratio of most skyscrapers)

With those values, we get $I_{motion\ based}$ being 4.7 times larger than $I_{strength\ based}$. This shows that with current materials being used, and for dimensions currently used for tall skyscrapers, if we design a building to withstand motion, it will also withstand strength. Therefore, motion based design is a very attractive approach as it allows to save time by only looking at motion constraints, which are the worst case scenario in tall buildings.

2.3 Mitigation of Wind-Induced Motion [19][31]

Many schemes have been developed in order to mitigate wind motion in tall buildings, which has become, as previously explained, the most important constraint. However because of the variety of solutions that have appeared, this paper will only list a few general categories of mitigation with a few examples for each.

2.3.1 Increasing Stiffness with an Efficient Structural System

The first way to mitigate motion in tall building is to increase stiffness in the building. This was of course used in old buildings, but also in the first skyscrapers. The Empire State Building, for example, which is a heavyweight skyscraper, deflects only 10.1 inches with an 80mph wind [19]. However with evolving materials, increasing the mass of the building to increase its stiffness is not a viable solution anymore. This is why engineers had to come up with efficient structural systems to resist wind loads.

2.3.1.1 Concrete Shear Walls

In this solution, concrete walls – called *shear walls* - are used from the foundation to the top of the building. Horizontal loads are carried through the floor to the shear walls, which then carry the load all the way to the ground. This provides a good overall lateral stiffness, but has the main disadvantage of obstructing a complete wall. Several schemes can be found to counteract this problem, such as using them as separating elements in apartments, or putting them as a central core near elevators and stairs in commercial buildings. This is also a poor scheme as it can only be used for moderately high buildings (40 stories tall), at which point too much material is required to make the building stiff enough.

2.3.1.2 Belt Trusses

The belt truss system is a scheme where the exterior columns are link together with a truss which is a few stories deep. This allows the lateral loads to be carried not only by the core and shear walls, but also by the exterior columns. This scheme allows building higher structures which can go up to 60 stories tall. The more belt trusses are used, the stiffer the system gets.

2.3.1.3 Tubular Systems

This evolution then led to a new type of system mainly developed in the 1970's by Fazlur Khan. This system consists of having very closely spaced exterior columns around the perimeter, in such a way that the whole building works as a hollow box. This greatly increases stiffness of a building, and many schemes can then be developed (trussed tube, bundled tube, tube inside a tube, etc.). Skyscrapers can go from 80 to 140 stories tall with this scheme, which was very popular.

2.3.2 Aerodynamics [32]

Although structural systems work well, they are more efficient for circular or square shaped buildings. Furthermore, the structural system usually becomes too apparent in certain buildings, mainly because the exterior part of the building is used for structural needs. With current evolution of architecture, new trends have come up, and architects are more prone to aerodynamics modification of buildings, where one changes the shape of the building in order to reduce wind effects on it. This allows more flexibility (more complex geometries) on the architectural design.

A first simple way of reducing wind effects on a structure is to slope the exterior façades, which lead to a reduction of 10 to 50% of the lateral drift [19]. This scheme can be used in a discrete way (tapering), by simply reducing the floor area as the building rises, like in Burj Khalifa in Dubai, or directly, like for the Shard in London (see Figure 2.13, which is not to scale).

Figure 2.13: Burj Khalifa (left) and The Shard (right), Both Using a Sloped System [2] (Not to Scale)

Another way to decrease wind effects on a building is to create *setbacks* to the cross sectional areas. This can be used as an architectural feature as to highlight the height of the building, but it reduces the wind effect as well. It was used on the JinMao tower in Shanghai, as well as on the Petronas Tower in Kuala Lumpur (See Figure 2.14). The more setbacks are made, and the more "sculptured" the building is at the top, the more efficient the wind reduction effect becomes.

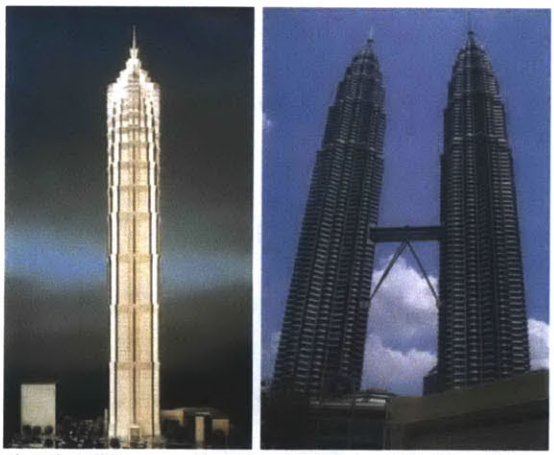

Figure 2.14: Setback Effect on JinMao (left) and Petronas Tower (right) [32]

Another way of reducing wind effect is to simply vary the geometry of the corners (Figure 2.15), which significantly reduces wind loads. In Taipei 101, corner modifications provided a 25% reduction in base moment (compared to the original square design). Additional studies have shown

that chamfers of 10% of the width gives a wind response reduction of 40% in the along wind, and 30% in the transverse wind.

However, more recent studies have also shown that modifying corners can sometimes have an adverse effect, increasing wind induced motion [26].

Figure 2.15: Corner Modifications [32]

Another scheme which was used in Shanghai World Financial Center is to have an opening at the top level, in order to significantly reduce vortex shedding effect. Again, although this method proves to be useful when creating an opening at the top of the building, it has also shown to worsen the effects when used on lower levels of the building.

2.3.3 Counteracting Forces

In certain cases, structural schemes and aerodynamic modifications are still not enough to mitigate wind induced motions in skyscrapers. Indeed, structural solutions can only reduce static loading, and as have been discussed in section 2.1.1, wind loads sometimes have a dynamic effect on structure. Although this dynamic effect can be reduced through aerodynamic effects, sometimes, this is not enough, and new schemes have since been developed to solve this issue. Unlike conventional solutions, these schemes make the structure respond dynamically to wind loads.

In dynamic problem, damping can be used as an effective solution to dissipate stored energy, since the structure has a certain velocity, unlike in static problems. One of the challenges today, however, is related to physical capacities of dampers. Damping ratio in civil engineering is still very low (from 2 to 5 or 10%), and costs a lot.

Another solution is to apply forces on the system which can counteract the negative effect of loadings. One example, which will be discussed in the next chapters, is the use of a mass, which in a dynamic scenario, provides an inertial force. If we manage to tune this force out of phase with the movement of the building (through the use of springs, which change the frequency of the mass), then it can act in the opposite movement of the building. These devices are generally known as Tuned Mass Dampers, although many various schemes have been developed since, resulting in new names such as Active Mass Dampers, Tuned Liquid Dampers etc.

Other types of force can also be used, mainly through actuators that activate accordingly to the position of the building. These schemes are called active schemes, and although they work well, they have a higher risk of failing. Indeed, in active schemes, sensors have to detect a critical configuration; information must then be sent to a control system, which must calculate the forces to apply; information has to be sent to the actuators, which must apply the forces. In this scenario, failure may come from the sensors, the control system, the actuators themselves, or even from the transmission system. However, even if they seem less secure, these schemes allow a much more responsiveness of the structure, making it a lot more efficient.

Chapter 3 - Tuned Mass Dampers

3.1 History of Tuned Mass Dampers [30]

A Tuned Mass Damper (TMD) is, as explained in section 2.3.3, an auxiliary system consisting of a mass, spring and damper, mounted in a structure. The mass provides inertial force ($-m\ddot{u}$), the spring provides a specific stiffness which consequently gives a specific frequency, allowing the Tuned Mass Damper to move out of phase with the building. This allows the total force (applied load + inertial force) to cancel out, leaving the structure intact. The damper is used to dissipate energy, so that the TMD doesn't oscillate back and forth indefinitely.

Frahm, in 1909 was the first to implement the concept of a Tuned Mass Damper, to reduce motion and vibrations in ships. Theory was later developed by Ormondroyd and Den Hartog in 1928 for a single degree of freedom system. They also presented afterwards a detailed discussion about optimal parameters for a TMD in 1940. Since then, significant extension in research has been made by Randall et al. (1981), Warburton (1981, 1982), Warburton and Ayorinde (1980), and Tsai and Lin (1993).

Table 3.1 shows a short list of buildings, adapted from [31], using "traditional" TMDs - as explained in section 3.2 - according to their date of construction. Several buildings however, required 2 to 3 TMDs in order to counteract movement in the x and y directions, and sometimes for the torsional mode. In such cases, the table only lists the TMD with the highest period. This is a non-exhaustive list.

Building	Use	Year	Height (m)	Building weight (tons)	TMD weight (tons)	Mass ratio	Building Period (s)	TMD Movement
CN Tower, Toronto	Tower	1975	553		20			
John Hancock, Boston	Office	1977	243.84		300			
Citicorp Building, New York	Office	1978	278		410			± 2.18m
Sydney Tower, Sydney	Tower	1981	305		180			± 15cm
Chiba port tower, Chiba	Tower	1986	125	1950	10	0.51%	2.25	
MHS Design Office, Tokyo	Office	1988	26.8		2.5		0.7	
Fukuoka Tower, Fukuoka	Office	1989	150.7	4000	30	0.75%	3.3	± 110cm
Higashiyama Sky Tower, Nagoya	Tower	1989	134	1960	19.8	1.01%	2.2	± 15cm
Crystal Tower, Osaka	Office	1990	157	44000	180	0.41%	3.6	± 25cm
Hibikiryokuchi Sky Tower, Kitakyushu	Observatory	1991	135					
Huis Ten Bosch Tower, Nagasaki	Tower	1992	105	4599	7.8	0.17%	1.75	± 80cm
ORC 200 Symbol Tower, Osaka	Office, Hotel	1992	200	56680	115	0.20%	4.72	± 50cm
Rokko-Island P&G, Kobe	Office	1993	131	27000	90	0.33%	2.94	
ACT Tower, Hamamatsu	Office, Hotel	1994	212	110000	90	0.08%	4.52	± 90cm
Akita Tower, Akita	Tower	1994	112.1	2186	15	0.69%	2.3	
Building M, Osaka	Residence, Office	1994	30.4	270	2.44	0.90%	0.75	± 2.6cm
Building S, Osaka	Office	1994	30.9		1		0.59	
Chifley Tower, Sydney	Office	1994	209	20000	400	2.00%		± 91cm
Hotel Ocean 45, Miyazaki	Hotel	1994	154.3	83650	120	0.14%	3.9	± 50cm
Sea Hawk Hotel, Fukuoka	Hotel	1995	143	42000	132	0.31%		
T Building	Office	1997	31.1	842	8.5	1.01%	0.81	
Washington National Airport Tower, USA	Tower	1997	67.5		9			
Sendai AERU	Multi-Purpose	1998	145.5	28750	100	0.35%		
Yoyogi 3-Chrome Kyodo Building	School	1998	89	80000	40	0.05%		

Table 3.1: List of buildings using a traditional TMD (adapted from [31])

Although Tuned Mass Dampers are designed specifically according to each building, this table gives a good estimate of general range of application of TMDs, such as:

- Mainly used in Offices and Towers, probably because as they take up a lot of space to move back and forth, architects do not like them that much.
- Applicable for a wide range of heights, going from 30m (8 stories) up to 550m.
- Applicable for a wide range of periods, going from 0.7s to 5s
- They weigh from 1 to 400 tons each (from 0.05% to 2% of the total mass of the building), and oscillate from a few centimeters to several meters.

Other interesting information which is not listed in the table is related to performance of Tuned Mass Dampers. In most case, they are designed to counteract wind loads, and rarely used to reduce earthquakes induced motions – only 4 cases in this table were designed for wind and earthquake. Results, when given, show that TMDs give an increase of 1 to 5% in damping ratio to the overall structure, and reduce building response to wind by 50% in most case (from 33% to 60%). The full table from [31] is given in Appendix 1.

3.2 Theory for a Single Degree of Freedom Tuned Mass Damper

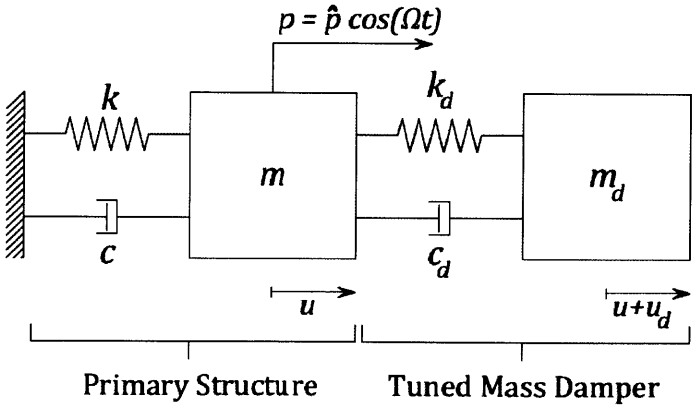

Figure 3.1: Single Degree of Freedom System with a Tuned Mass Damper

Let us consider a very simple model of a structure with a TMD attached to it, as depicted in Figure 3.1. The building structure is modeled by a simple one degree of freedom system, to which a force (wind) is applied [30]. For ease of analysis, we shall assume a periodic loading.

Firstly, we define the properties of the building alone.

m	Mass of the Building alone
k	Stiffness of the Building alone
c	Damping of the Building alone
$\omega = \sqrt{\frac{k}{m}}$	Natural frequency of Building alone
$\xi = \frac{c}{2m\omega}$	Damping ratio
u	Displacement of the building
$p = \hat{p}\cos(\Omega t)$	Harmonic load applied on the building (Wind for example)

We also define with subscript "d" everything that is related to the Tuned Mass Damper:

m_d	Mass of the Tuned Mass Damper
k_d	Stiffness of the Tuned Mass Damper
c_d	Damping of the Tuned Mass Damper
$\omega_d = \sqrt{\frac{k}{m}}$	Natural frequency of Tuned Mass Damper
$\xi_d = \frac{c_d}{2m_d\omega_d}$	Damping ratio of the Tuned Mass Damper
u_d	Relative displacement of the Tuned Mass Damper

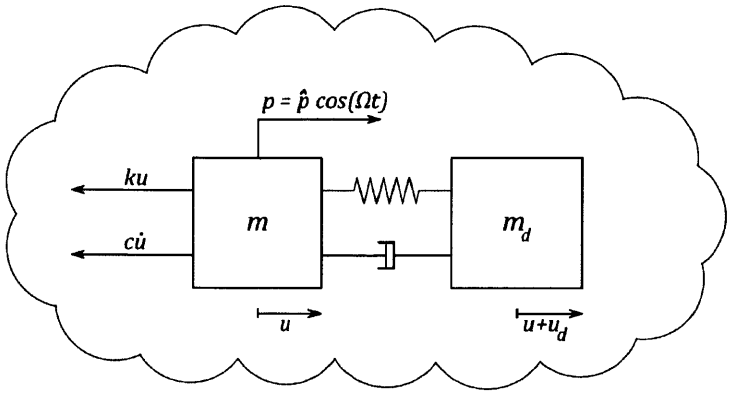

Figure 3.2: Free Body Diagram of the Structure with a Tuned Mass Damper

The free body diagrams (Figure 3.2 and Figure 3.3) allow us to derive the two governing equations of the system, through Newton's second law ($\sum F = m\ddot{u}$).

$$m\ddot{u} + m_d(\ddot{u} + \ddot{u}_d) + c\dot{u} + ku = p \tag{3.1}$$

We define the mass ratio

$$\bar{m} = \frac{m_d}{m}$$

Dividing equation (3.1) by m, and rearranging the terms gives us the first equation of motion

$$(1 + \bar{m})\ddot{u} + \bar{m}\ddot{u}_d + 2\xi\omega\dot{u} + \omega^2 u = \frac{p}{m} \tag{3.2}$$

Similarly, we look at the Tuned Mass Damper's free body diagram (Figure 3.3) to derive the second governing equation

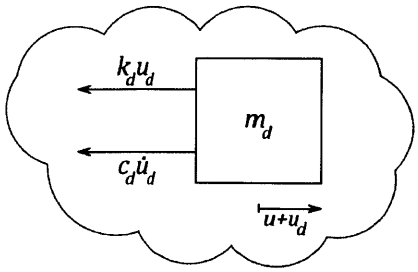

Figure 3.3: Free Body Diagram of the Tuned Mass Damper Only

$$m_d(\ddot{u} + \ddot{u}_d) + c_d\dot{u}_d + k_d u_d = 0 \tag{3.3}$$

Dividing equation (3.3) by m_d, and rearranging the terms gives us the second equation of motion

$$\ddot{u} + \ddot{u}_d + 2\xi_d\omega_d\dot{u}_d + \omega_d^2 u_d = 0 \tag{3.4}$$

We define Mass, Damping and Stiffness Matrices respectively

$$\underline{M} = \begin{pmatrix} 1+\bar{m} & \bar{m} \\ 1 & 1 \end{pmatrix} \qquad \underline{C} = \begin{pmatrix} 2\xi\omega & 0 \\ 0 & 2\xi_d\omega_d \end{pmatrix} \qquad \underline{K} = \begin{pmatrix} \omega^2 & 0 \\ 0 & \omega_d^2 \end{pmatrix}$$

as well as Displacement and Force matrices. For ease of calculations, we use complex notations

$$\underline{U}(t) = \begin{pmatrix} u(t) \\ u_d(t) \end{pmatrix} = \begin{pmatrix} \hat{u}(\Omega) \\ \hat{u}_d(\Omega) \end{pmatrix} e^{i\Omega t} = \underline{\hat{U}}(\Omega)e^{i\Omega t} \qquad \underline{P}(t) = \begin{pmatrix} p(t)/m \\ 0 \end{pmatrix} = \begin{pmatrix} \hat{p}/m \\ 0 \end{pmatrix} e^{i\Omega t} = \underline{\hat{P}}e^{i\Omega t}$$

Which we can write in matrix form

$$\underline{M}\,\ddot{\underline{U}} + \underline{C}\,\dot{\underline{U}} + \underline{K}\,\underline{U} = \underline{P} \tag{3.5}$$

When replacing $\underline{U}$ and $\underline{P}$ with their complex notation, and dividing by $e^{i\Omega t}$ equation (3.5) comes to

$$\left(-\Omega^2\underline{M} + i\Omega\underline{C} + \underline{K}\right)\underline{\hat{U}} = \underline{\hat{P}} \tag{3.6}$$

We define

$$\underline{Z} = \left(-\Omega^2\underline{M} + i\Omega\underline{C} + \underline{K}\right)$$

$$\underline{Z} = \begin{pmatrix} -\Omega^2(1+\bar{m}) + 2i\Omega\xi\omega + \omega^2 & -\Omega^2\bar{m} \\ -\Omega^2 & -\Omega^2 + 2i\Omega\xi_d\omega_d + \omega_d^2 \end{pmatrix}$$

We also define the inverse matrix of $\underline{Z}$

$$\underline{Z}^{-1} = \underline{H} = \begin{pmatrix} H_{11} & H_{12} \\ H_{21} & H_{22} \end{pmatrix}$$

According to equation (3.6)

$$\underline{\hat{U}} = \underline{H}\,\underline{\hat{P}}$$

Therefore, we are only interested in H_{11}, which gives the response $\hat{u}(\Omega)$ of the building due to a load applied on the primary structure. Indeed, in the model we are looking at, we are only interested in the displacement of the main structure (even if movement of the Tuned Mass Damper is an issue, we aren't focusing on this aspect for now). Moreover, the load is considered to be applied on the main

structure only, as we consider the Tuned Mass Damper to be inside the building, and not being moved by the wind loads.

$$\hat{u} = \hat{p}H_{1,1}$$

$H_{1,1}$'s literal expression is derived through MATLAB® [1], and expressed in terms of the following unit less properties:

$\overline{m} = \frac{m_d}{m}$ Mass ratio

$f = \frac{\omega_d}{\omega}$ Frequency ratio (of Tuned Mass Damper)

$\rho = \frac{\Omega}{\omega}$ Frequency ratio (of forcing function)

For ease of reading, we pick the case where the building has no damping ($\xi = 0$):

$$H_{1,1} = \frac{[f^2 - \rho^2 + 2i\xi_d\rho f]}{k\{[1 - \rho^2][f^2 - \rho^2] - \overline{m}\rho^2 f^2 + 2i\xi_d\rho f[1 - \rho^2(1 + \overline{m})]\}} \tag{3.7}$$

$H_{1,1}$ can be also expressed in terms of mass, stiffness and damping if needed [33]:

$$H_{1,1} = \frac{[k_d - \Omega^2 m_d + i\Omega c_d]}{k\left[1 - \frac{\Omega^2(m_d + m)}{k}\right]\left[k_d - \frac{(k - \Omega^2 m)\Omega^2 m_d}{k - \Omega^2(m_d + m)} + i\Omega c_d\right]} \tag{3.8}$$

We are only interested here in the amplification factor of the dynamic load. Therefore, we have to analyze the absolute value of the response $\hat{u}$ divided by the static deflection $\frac{\hat{p}}{k}$. The amplification factor ($A = \left|\frac{H_{1,1}}{k}\right|$) is plotted against the frequency ratio in Figure 3.4, for random initial mass and stiffness values. The amplification factor is plotted for 50 equally incremented values of damping ratios (of the TMD). As can be seen from the plot, the system goes from a 2 degree of freedom system ($\xi_d = 0$, two harmonic frequencies) to a 1 degree of freedom system ($\xi_d = \infty$, one harmonic frequency). Another interesting fact to note is the existence of two points P and Q, through which all plot will pass, no matter what the damping ratio.

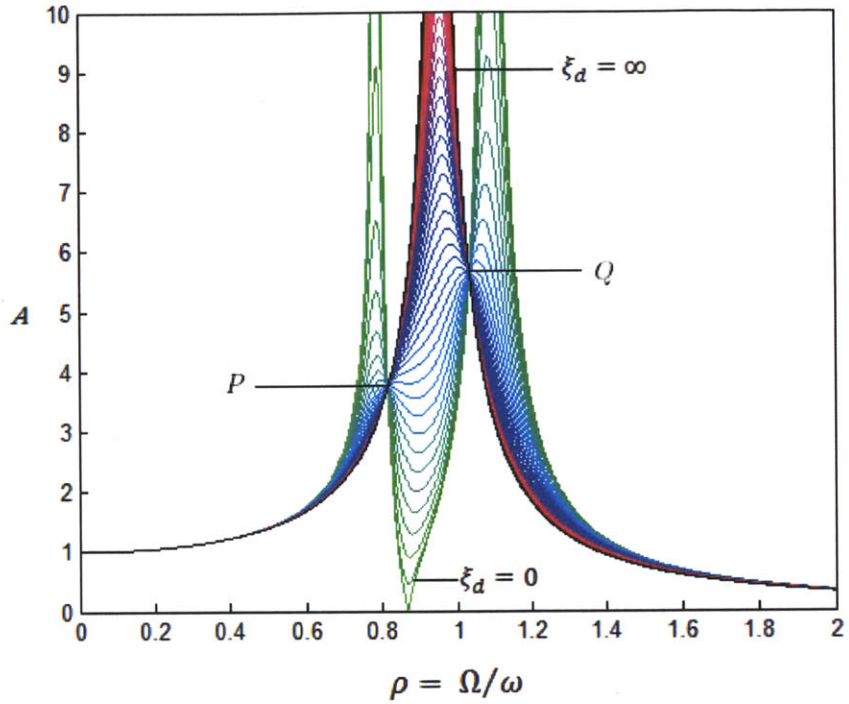

Figure 3.4: Amplification Factor of the Building versus Frequency Ratio (Untuned Damper)

Mathematically, this can be explained by looking at equation (3.8). For specific values of Ω, part of the numerator and denominator can cancel out [33], removing the imaginary component of the equation. This is achieved when

$$[k_d - \Omega^2 m_d + i\Omega c_d] = \pm\left[k_d - \frac{(k - \Omega^2 m)\Omega^2 m_d}{k - \Omega^2(m_d + m)} + i\Omega c_d\right] \tag{3.9}$$

If equation (3.9) is satisfied, equation (3.8) comes to

$$H_{1,1} = \frac{\pm 1}{k\left[1 - \frac{\Omega^2(m_d + m)}{k}\right]} \tag{3.10}$$

This shows that, for these specific values $\Omega_{P,Q}$, $H_{1,1_{P,Q}}$ is independent of c_d, and each plot, no matter what the damping ratio is, will go through these points $(\Omega_P, H_{1,1_P})$ $(\Omega_Q, H_{1,1_Q})$. These values, however, depend on the stiffness and mass of the prime structure and TMD. Therefore, assuming the building has fixed values, and the TMD can be designed accordingly, by modifying the values of m_d and k_d, we can change the position of points P and Q. A simple analysis of Figure 3.4 makes us

understand that P and Q will be the maximum amplifications for the optimum configuration. More in depth analysis shows that this optimum value is obtained for $H_{1,1_P} = H_{1,1_Q}$. This is shown in Figure 3.5.

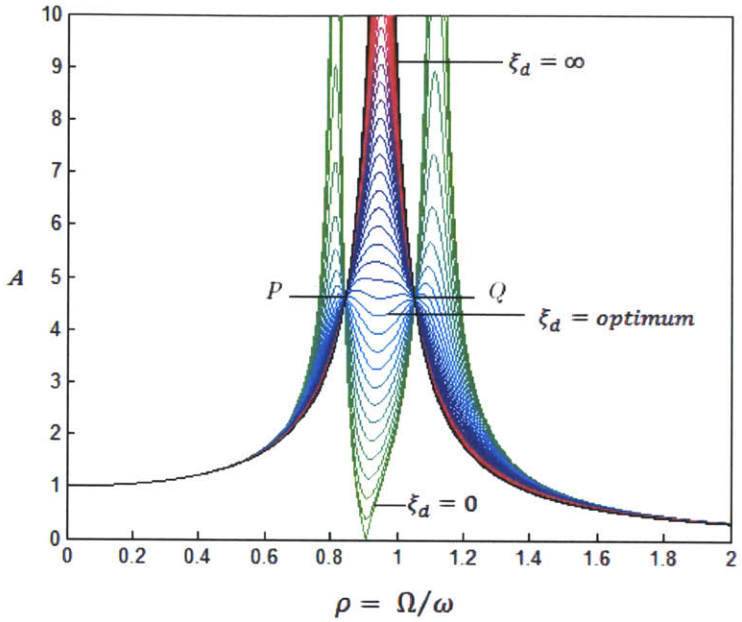

Figure 3.5: Amplification Factor of the Building versus Frequency Ratio (Tuned Damper)

3.3 Efficiency of Tuned Mass Dampers

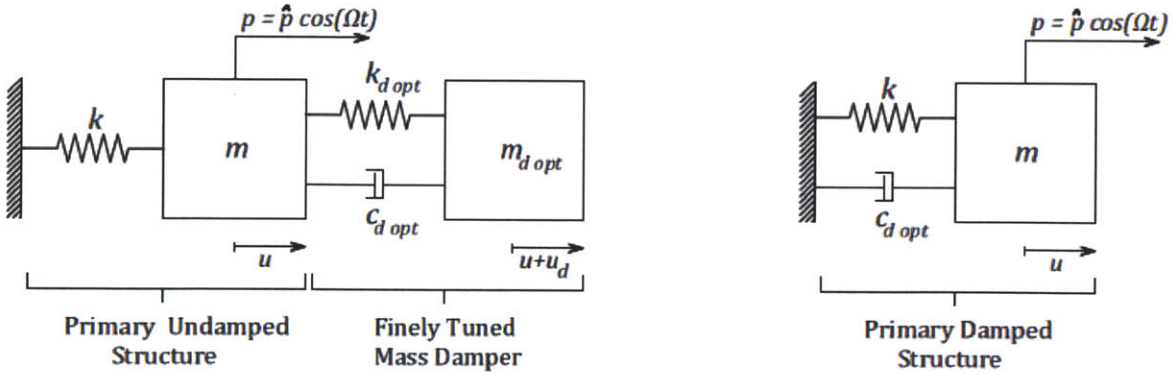

Figure 3.6: Undamped Structure with TMD versus Damped Structure Without TMD

To make sure the TMD system is effective, we can compare the amplification factor between two systems: 1) an undamped structure with a finely tuned mass damper (optimal mass, stiffness and damper) and 2) a structure damped with the optimally calculated damper from the 1st system, as depicted in Figure 3.6.

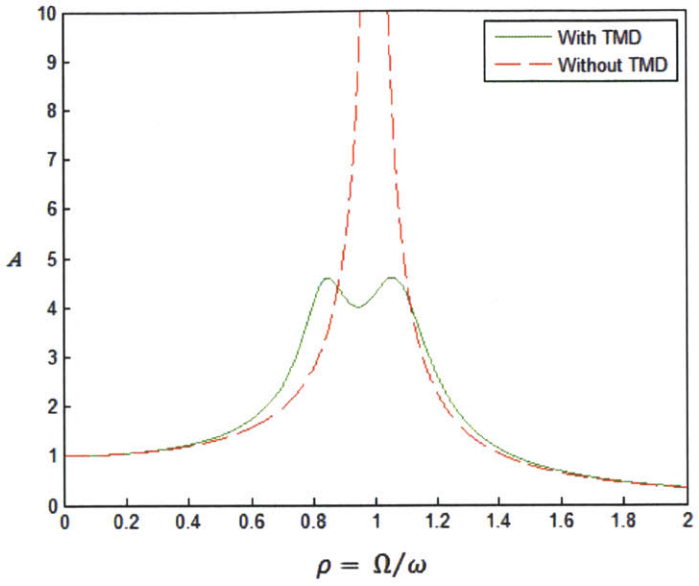

Figure 3.7: Dynamic Amplification of a 1 DOF system With and Without a TMD

Figure 3.7 compares the amplification function for each system. Two conclusions can be made from the results. Firstly, the added tuned mass damper does help reduce the dynamic response of the structure (on actual structures, measurements have shown to reduce response by 30 to 50%, which agrees with Figure 3.7 for excitations near harmonic excitations (for $\rho \approx 1$, A goes from 8-9 to 4-5).

However, the effect of the added TMD is significant for a very slight range of frequencies (roughly for ratios between .6 and 1.2). Therefore, if the exciting frequency is not near the natural frequency of the building, the TMD will have no effect. Furthermore, if a structure suffers damage, its stiffness will decrease, and the TMD won't be tuned to the right frequency anymore. This can be seen in Figure 3.8, in which the primary structure's stiffness incrementally decreases, while the TMD's properties remain constant.

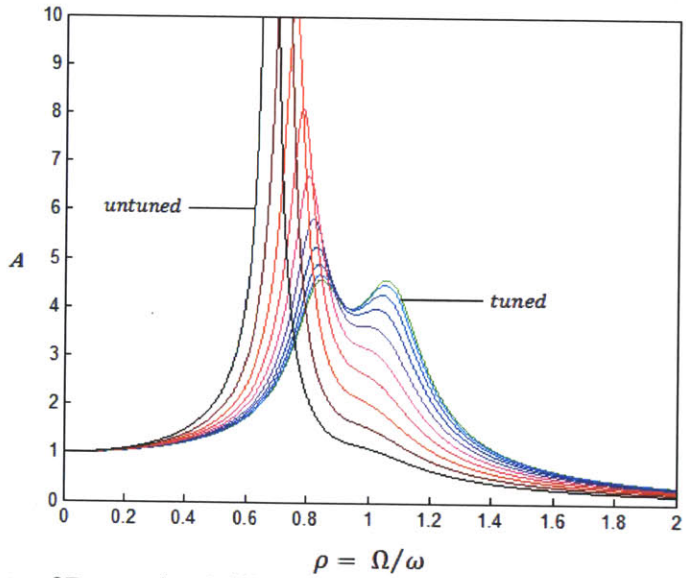

Figure 3.8: Effects of Decreasing Stiffness in Primary Structure on Dynamic Amplification

3.4 Types of Tuned Mass Damper [31]

As discussed in the previous section, one of the first limitations of Tuned Mass Dampers is the fact that they are only tuned to a specific frequency. Other drawbacks – which will further be discussed – have led engineers to develop new dampers to overcome those limitations. A short list of dampers schemes will be discussed in this section.

3.4.1 Activity

Whatever the type of damper used, they can always be more or less active. Four schemes have currently been developed, as illustrated in Figure 3.9. In each of the schemes, (m, k, c) represent the main structure's properties, (m_d, k_d, c_d) the damper's properties, (a) the actuators, (s) the sensors, and $(cont)$ the control system.

3.4.1.1 Passive Dampers (TMD)

As presented in section 3.2, these dampers were the first scheme developed. They are tuned to a specific frequency, with fixed properties (mass, stiffness and damper) which cannot change. This has two effects: on the one hand, they are only effective for a specific range of frequencies, on the other

hand however, because they can't change properties, they are very reliable for these specific frequencies, and there is no risk of worsening the effect.

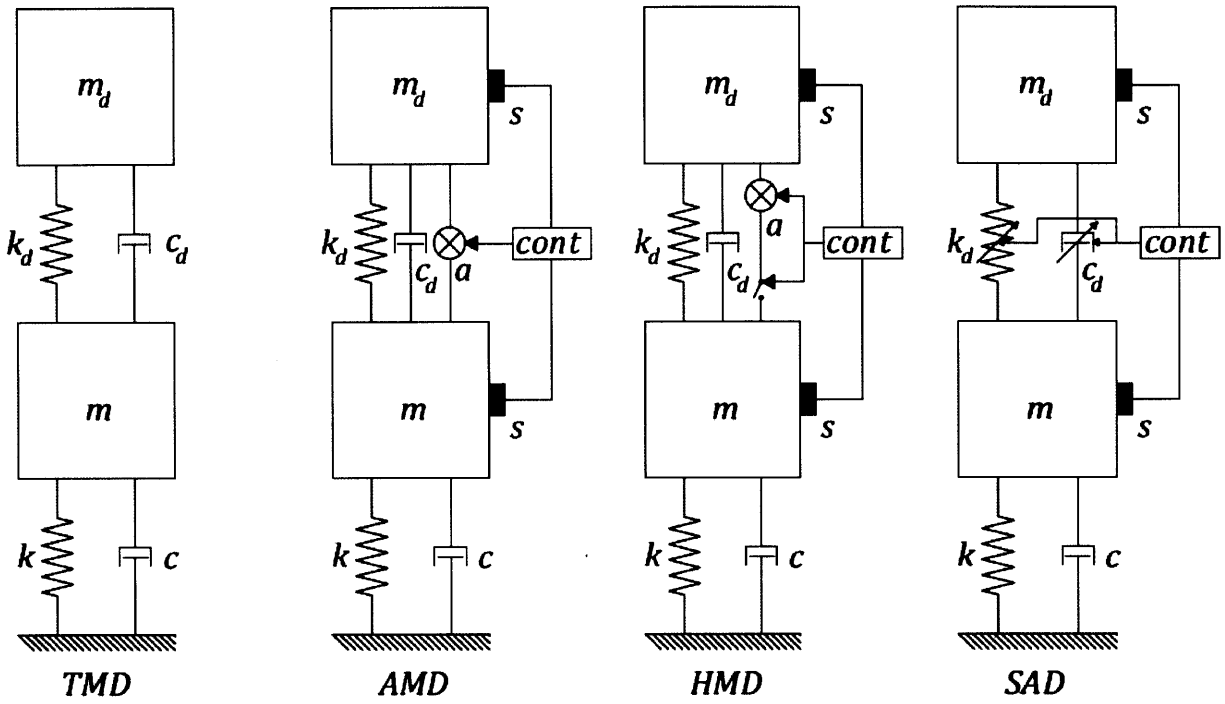

Figure 3.9: Types of Dampers According to Their Adaptability (Adapted from [31])

3.4.1.2 Active Dampers (AMD)

Usually called Active Mass Dampers (AMD), these systems were developed to compensate for the tuning frequency. They are comprised of a fixed mass, spring and damper (like the TMD) and an active system (sensors + controller + actuator). The active part allows the system to apply a variable force which can change the response of the damper when frequency of excitation changes. In order to do this, sensors can be put on the structure to monitor its movement, or to measure the load applied on it. The controller will then calculate the required force to counteract the movement of the building, and activate the actuator accordingly. This allows the system to resist dynamic forces for a much wider range of frequencies. Another sensor can be put on the AMD, for example to measure its velocity and apply a force proportional to it, resulting in an increase in damping.

However, this system has a few drawbacks. First of all, because it is an active system, it is not as reliable as the passive system. Indeed, failure may occur at the sensors (wrong readings), at the controller (wrong code), at the actuator (wrong force applied) or even through transmission (broken wires). Furthermore, electricity shortage can cause failure of the whole system. A second risk (less probable) of this poor reliability is that instability may occur if the AMD responds wrongly to the forcing function, or not quick enough.

The second major drawback of this system is the fact that it requires considerable amount of energy to provide sufficient response. Therefore, not only is the installation cost more expensive than a regular TMD (due to the addition of the active control system) but maintenance and energy cost drastically rise. This is especially true for AMD which only use an actuator and a mass (no spring or damper is used), in which case the force required is very important.

3.4.1.3 Hybrid Dampers (HMD)

Another type of damper, the Hybrid Mass Damper (HMD), was then developed in order to take advantage of both the passive and the active schemes. The damper in this system can work either as an active damper, or as a passive damper, according to the loading. This provides a good compromise of both systems.

Firstly, HMD are less prone to instability risks than AMD: as soon as the structure detects an event where an AMD scheme could cause failure, the system can switch to the passive TMD. Second, HMD cost less than an AMD scheme because the actuator is not constantly in use, reducing energy cost. Third, because HMD can apply a force, they still have a way to vary the range of frequencies for which they are efficient.

3.4.1.4 Semi-Active Dampers (SAD)

The last type of damper is called a Semi-Active Damper (SAD). It is called an Active system because an active control system still exist (sensors + controller). However in this scheme the spring and damper have variable properties, which can be changed with minimal use of energy, hence the term Semi. In this scheme, there are no more actuators, and the adaptability of the damper is made through variation of stiffness and damping properties.

The limitations in this scheme are the capabilities of such springs and dampers. In civil engineering, very few schemes have been developed to greatly vary the stiffness or damping. These schemes usually use more recent technologies, such as magneto rheological dampers, which allow for more variations.

3.4.2 Form

Two other major drawbacks of the TMD, whichever the activity, are the horizontal space required, as well as the weight of the device. Not only does the mass takes up space, but also because it requires area to sway back and forth. Therefore many schemes have been developed in order to remove this drawback.

3.4.2.1 Pendulum [30]

Hanging a mass inside a building provides (see Figure 3.10, left) the same effect as a TMD. This scheme allows for a simpler design of the TMD's bearings, which are sometimes complicated. Although this scheme is attractive, it usually requires a considerable amount of vertical space in order to increase the effectiveness. In Taipei 101 for example (see section 1.3.2.1), the pendulum requires 4 floor heights, and it is used as an attraction site in order to compensate for this major drawback.

In terms of equation of motion, the pendulum works like a simple TMD, where the damper stiffness and frequency are given by:

$$k_d = \frac{m_d \times g}{L} \qquad \omega_d = \sqrt{\frac{g}{L}}$$

where $g = 9.81\ \mathrm{m.s^{-2}}$ is the acceleration of gravity.

Damping can be added to the pendulum, by attaching a damper between the mass and the lower floor, as was done on Taipei 101. The matrices become:

$$\underline{M} = \begin{pmatrix} 1+\bar{m} & \bar{m} \\ 1 & 1 \end{pmatrix} \qquad \underline{C} = \begin{pmatrix} 2\xi\omega & 0 \\ 0 & 2\xi_d\sqrt{\frac{g}{L}} \end{pmatrix} \qquad \underline{K} = \begin{pmatrix} \omega^2 & 0 \\ 0 & \frac{g}{L} \end{pmatrix}$$

Compound pendulums schemes (see Figure 3.10, right) have also been developed to reduce height. In this case, the effective length becomes nL, where n is the number of levels in the compound pendulum. For example, in Figure 3.10, the damper's stiffness is $k_d = \frac{m_d \times g}{2L}$.

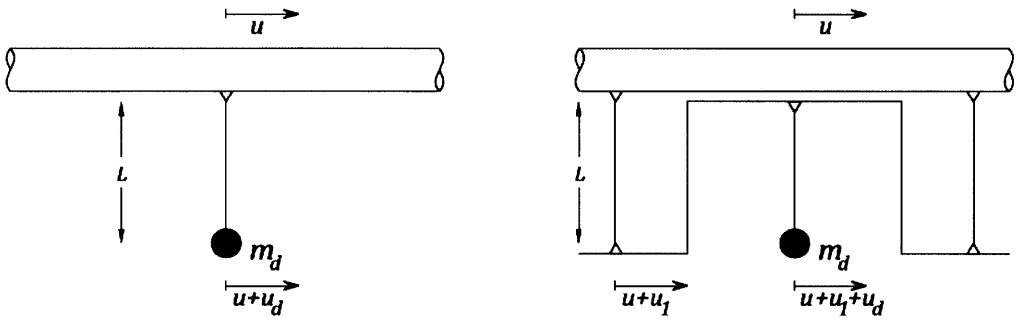

Figure 3.10: Simple Pendulum (left) versus Compound Pendulum (right) Scheme [30]

3.4.2.2 Liquid Dampers (TLD) [31][34]

Another type of dampers has been developed, where the role of the mass is replaced by the use of a liquid material. These Tuned Liquid Dampers (TLD) were first tried on structures in the 1980's and present several advantages to regular TMDs. Firstly, liquid dampers require relatively low cost and maintenance. A second, more interesting feature to buildings is that the water used in TLDs can also be used as building water supply. Therefore, it is sometimes possible with this scheme to provide additional damping, without adding any supplementary mass, by simply using existing water tanks.

Liquid Dampers can be separated into two categories, according to the water container: large tanks of water, commonly called *sloshing dampers* (discussed in section 3.4.2.2.1), or more slender tubes, known as *liquid column dampers* (discussed in section 3.4.2.2.2).

3.4.2.2.1 Sloshing Dampers (TSD) [35]

Tuned Sloshing Dampers (TSD) are schemes were a large tank of water is used as a TMD. Properties of the damper depend on the size of the water tank, which are labeled in Figure 3.11: given a direction of excitation, we define

L the length of the tank parallel to the direction of excitation
b the length of the tank perpendicular to the direction of excitation
h the depth of water

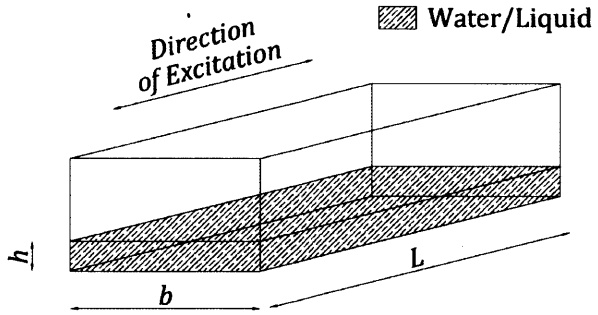

Figure 3.11: TSD Tank Properties (adapted from [35])

Two sub-categories have been defined in sloshing dampers, according to the h/L ratio: if it is less than 0.15, the category is known as *shallow-water* TSD; in the other case, they are called *deep-water* TSD. It is therefore possible for a TSD to act as a shallow TSD in one direction and as a deep TSD in the perpendicular direction.

In the shallow category, damping is provided through internal viscous forces of the fluid – i.e. fluid movement - as well as wave breaking. In the deep-water case, screens or baffles can be added to provide additional damping. However a large part of the water will not provide sloshing, thus only increasing the structure's mass.

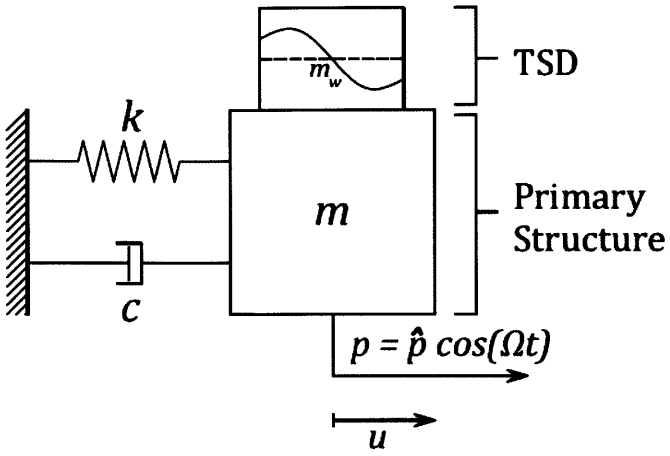

Figure 3.12: Model of a 1 DOF System With a Deep TSD (adapted from [35])

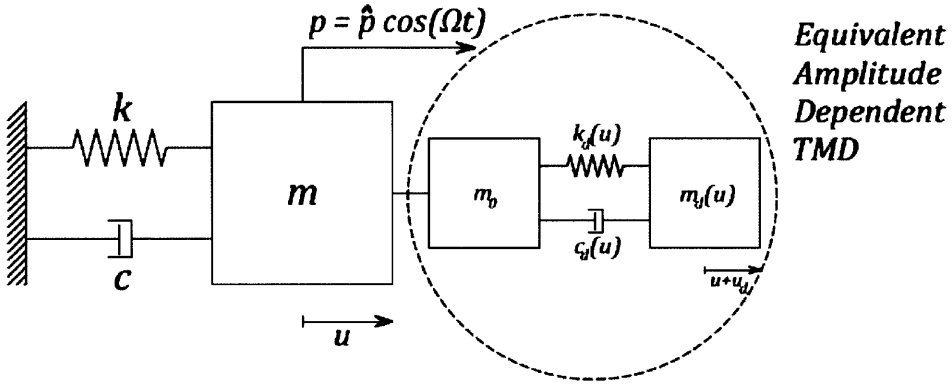

Figure 3.13: Proposed Model of an Equivalent TMD for the Deep TSD (Adapted from [35])

Figure 3.12 and Figure 3.13 present the model proposed by Tait et al. of a deep sloshing damper and its equivalent TMD. As is depicted, part of the mass of the water (m_0) does not participate in the sloshing, and is therefore an added mass to the structure. The rest of the properties of the TMD (m_d, k_d, c_d) are function of the displacement (u) of the structure. The equivalent TMD properties are as follows:

$$\omega_d = \sqrt{\frac{\pi g}{L}\tanh\left(\frac{\pi h}{L}\right)} \quad \text{(derived from linear wave theory)}$$

$$\xi_d = \frac{1}{2h}\sqrt{\frac{2\nu}{\omega_d}}\left(1+\frac{h}{b}\right) \quad \text{(where } \nu \text{ is the liquid kinematic viscosity)}$$

And the matrices become:

$$\underline{M} = \begin{pmatrix} 1+\bar{m} & \bar{m} \\ 1 & 1 \end{pmatrix} \qquad \underline{C} = \begin{pmatrix} 2\xi\omega & 0 \\ 0 & \frac{1}{h}(1+\frac{h}{b})\sqrt{2\nu\omega_d} \end{pmatrix} \qquad \underline{K} = \begin{pmatrix} \omega^2 & 0 \\ 0 & \frac{\pi g}{L}\tanh\left(\frac{\pi h}{L}\right) \end{pmatrix}$$

However, this is just one of the many models proposed for TSD, and an exact model has not yet been fully developed. Other models have been suggested, such as a multiple spring dampers or impact dampers.

3.4.2.2.2 Column Dampers (TLCD) [34]

Like TSD, Tuned Liquid Column Dampers (TLCD) uses fluid as the mass of the damper. However, unlike them, the tank is deformed into a tube-like shape, as illustrated in Figure 3.14.

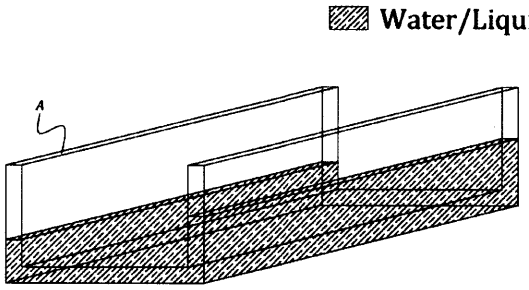

Figure 3.14: TLCD Tube

TLCD offers quite a few additional advantages compared to TSD:

- A mathematical model exists, therefore tuning of the TLCD can be precise
- An orifice can be put in the horizontal part of the tube in order to provide variable damping, with minimal energy input, thus allowing for semi-active systems.
- The tube's shape can be modified, making TLCD very flexible to architects' needs.

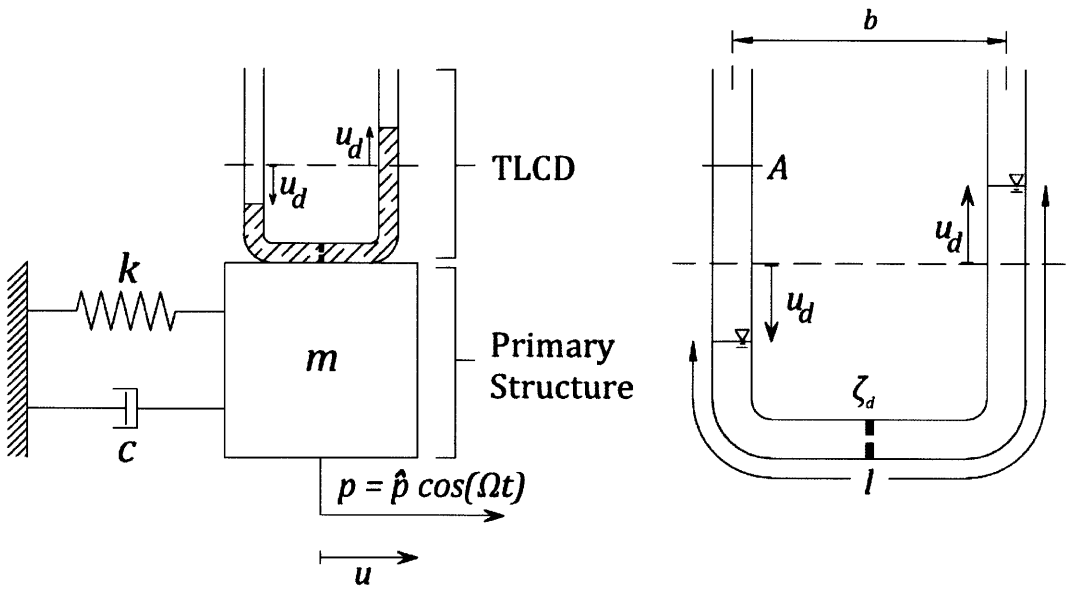

Figure 3.15: TLCD Model With Structure (left) and Alone (right) (Adapted from [34])

Figure 3.15 shows the model of a 1 DOF system with a TLCD, where we define:

A as the cross sectional area of the tube
b as the horizontal length of the liquid column
l as the total length of the liquid column
$\alpha = b/l$ as the length ratio
ρ as the mass density of the fluid
u_d as the vertical displacement of the liquid from its rest position
ζ_d as the head loss coefficient, which can be easily varied to obtain a semi-active system

The equations of motion for the structure and the TLCD respectively are given by [34]:

$$(m + \rho Al)\ddot{u} + \rho Ab\ddot{u}_d + c\dot{u} + ku = p \tag{3.11}$$

$$\rho Al\ddot{u}_d + \frac{1}{2}\rho A\zeta_d|\dot{u}_d|\dot{u}_d + 2\rho A g u_d = -\rho Ab\ddot{u} \tag{3.12}$$

Dividing equation (3.11) by m and equation (3.12) by ρAl, the matrices come to:

$$\underline{M} = \begin{pmatrix} 1 + \bar{m} & \alpha\bar{m} \\ \alpha & 1 \end{pmatrix} \qquad \underline{C} = \begin{pmatrix} 2\xi\omega & 0 \\ 0 & \frac{\zeta_d|\dot{u}_d|}{2l} \end{pmatrix} \qquad \underline{K} = \begin{pmatrix} \omega^2 & 0 \\ 0 & \frac{2g}{l} \end{pmatrix}$$

3.4.2.3 Others [36]

Other forms of TMD have also been developed, as is illustrated in Figure 3.16, but will not be discussed in this paper.

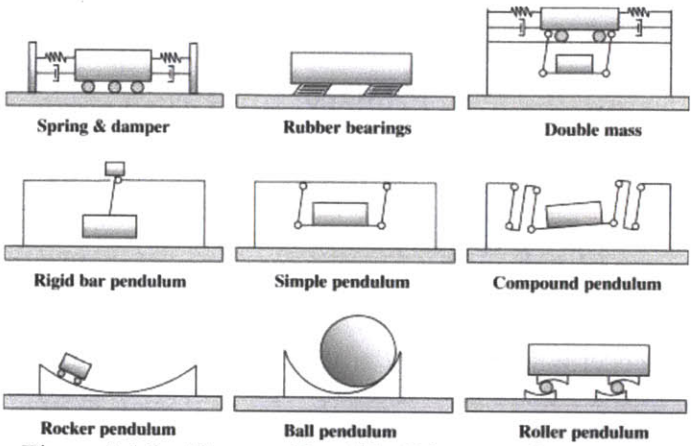

Figure 3.16 : Alternate Possible Schemes of TMD [36]

Chapter 4 - Effects of Tuned Mass Dampers

In this part of the paper, we try to analyze the response of a structure to various types of loadings. As an approximation, we can assume a structure is a one degree of freedom, in order to be close to the theory model of a TMD. This is explained in section 4.1.

4.1 Simplification of a Structure to a Single Degree of Freedom System

Unlike was has been presented earlier, a structure is actually not a single degree, but rather an infinite degree of freedom system. It is however, mathematically possible to simplify the structure's model; a first approximation requires to use the lumped mass model, where the model goes from an infinite to a multiple (finite) degree of freedom system. This is achieved by considering each floor is a single DOF, where the mass is the total mass of the considered floor, and the stiffness and damping are calculated using equivalence formulas – which depend on the properties of elements (EI, c), the fixations at the end (pinned, fixed) etc.

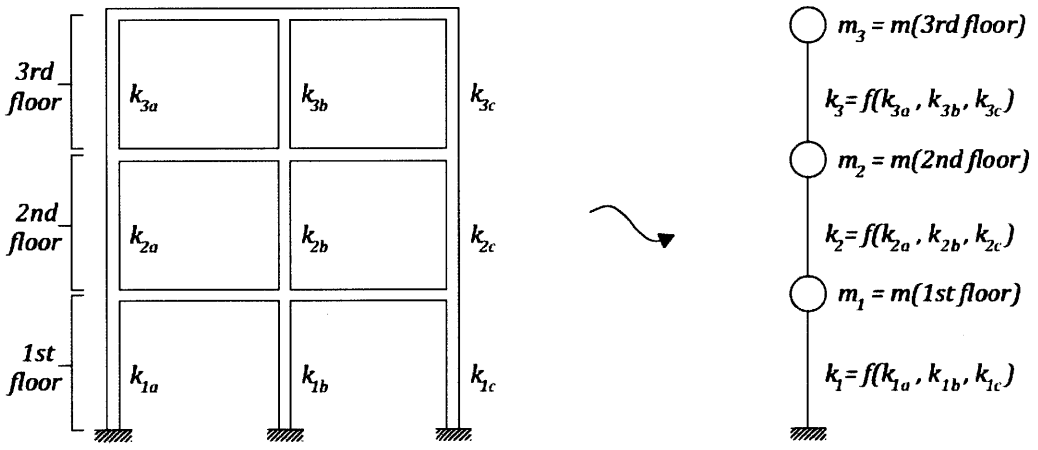

Figure 4.1: Lumped Mass Model Example for a 3-Story Building

Figure 4.1 gives a very simple example of how a building can be modeled as a 3 DOF system. This approximation is a pretty good one, as long as the formulas used to find equivalent stiffness and damping are precise enough. The lumped mass model can further be simplified; however an important assumption must be made: we must consider the movement to be harmonic – which is true when the

excitation is too, for example. If that is the case, another assumption must be made in order to simplify the mathematical problem: we have to consider the undamped case. In the same way we derived equation (3.5), we can calculate the mass matrix and stiffness matrix of the structure (damping matrix is considered void). For the specific example given in Figure 4.1, we get:

$$\underline{M} = \begin{pmatrix} m_1 & 0 & 0 \\ 0 & m_2 & 0 \\ 0 & 0 & m_3 \end{pmatrix} \qquad \underline{K} = \begin{pmatrix} k_1 + k_2 & -k_2 & 0 \\ -k_2 & k_2 + k_3 & -k_3 \\ 0 & -k_3 & k_3 \end{pmatrix}$$

Because the displacement is considered harmonic, we can write it as

$$\underline{U}(t) = \begin{pmatrix} u_1(t) \\ u_2(t) \\ u_3(t) \end{pmatrix} = \begin{pmatrix} \hat{u}_1(\Omega) \\ \hat{u}_2(\Omega) \\ \hat{u}_3(\Omega) \end{pmatrix} e^{i\Omega t} = \underline{\hat{U}}(\Omega) e^{i\Omega t} = \underline{\phi} q(t)$$

Where $\underline{\phi} = \underline{\hat{U}}(\Omega)$ is called the *modal shape* and $q(t) = e^{i\Omega t}$. For the free vibration problem (no external load applied), equation (3.5), which is the equation of motion, comes to:

$$\left(-\Omega^2 \underline{M} + \underline{K}\right)\underline{\phi} q(t) = 0 \tag{4.1}$$

The equation of motion being true at any given time t, equation (4.1) becomes

$$\left(-\Omega^2 \underline{M} + \underline{K}\right)\underline{\phi} = 0 \tag{4.2}$$

which is an Eigen value problem, and is solved for n specific pairs of $(\Omega, \underline{\phi})$, where n is the size of the matrices which is the same as the number of degrees of freedom of the system. Ω is also known as the *modal frequency*. Each pair of modal frequencies and modal shapes is gives a different solution, and results associated with that pair are called *modes*, arranged in decreasing order of modal frequencies. We will note Ω_i and $\underline{\phi_i}$ the modal properties related to the i^{th} mode In this case, for example, we will get 3 modes.

For a given mode i (i.e. a given modal frequency Ω_i and modal shape $\underline{\phi_i}$), the general equation of motion can be multiplied by $\underline{\phi_i}^T$:

$$\underline{M}\underline{\phi}_i\ddot{q}(t) + \underline{C}\underline{\phi}_i\dot{q}(t) + \underline{K}\underline{\phi}_i q(t) = \underline{P}(t) \tag{4.3}$$

$$\rightarrow \quad \left[\underline{\phi}_i^T \underline{M}\underline{\phi}_i\right]\ddot{q}(t) + \left[\underline{\phi}_i^T \underline{C}\underline{\phi}_i\right]\dot{q}(t) + \left[\underline{\phi}_i^T \underline{K}\underline{\phi}_i\right] q(t) = \underline{\phi}_i^T \underline{P}(t) \tag{4.4}$$

Because of the sizes of the matrices, all terms defined below are scalars:

$\left[\underline{\phi}_i^T \underline{M}\underline{\phi}_i\right] = \tilde{m}_i$ is the *modal mass*

$\left[\underline{\phi}_i^T \underline{C}\underline{\phi}_i\right] = \tilde{c}_i$ is the *modal damping*

$\left[\underline{\phi}_i^T \underline{K}\underline{\phi}_i\right] = \tilde{k}_i$ is the *modal stiffness*

$\left[\underline{\phi}_i^T \underline{P}\right] = \tilde{p}_i$ is the *modal force*

Furthermore, $q(t)$ being a scalar as well, equation (4.4) is actually a single degree of freedom problem, where the properties of the system are the modal values defined above.

$$\tilde{m}_i\ddot{q}(t) + \tilde{c}_i\dot{q}(t) + \tilde{k}_i q(t) = \tilde{p} \tag{4.5}$$

Therefore, for each mode, a structure can be modeled as a single DOF, as depicted in Figure 4.2. However, it is important to pick the right mode to convert the model to a single DOF system. It can be mathematically shown [33] that the modal frequencies Ω_i are the natural frequencies of the building, and therefore associated with the largest response of the structure. Since TMDs are used, in general, to reduce vibration induced by worst excitation, they are usually designed for a specific mode, which is the one chosen to simplify the model.

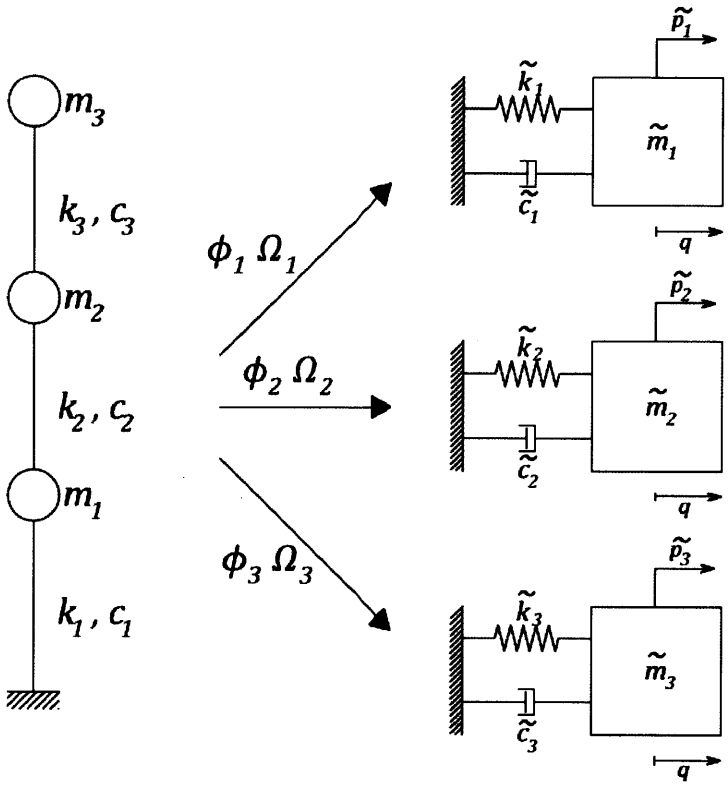

Figure 4.2: Conversion from a Lumped Mass Model to a Single DOF Model

Although to go from a whole structure to a single degree of freedom system we require several key assumptions, we will be assuming, for the rest of this paper, that such a conversion is possible. Therefore, the whole process of the simulation will be based on the response of a single DOF system with a TMD to various types of loading.

4.2 Simulation Principle

We try implementing, in the following pages, a way to approximately compute the displacement of the structure, given a 1 DOF system - on which is applied a load p (variable in the code) - with a TMD attached. We assume, in this problem, that the structure's and the TMD's properties are given, as well as the forcing function. Given the properties of the system, we can first compute the acceleration of the system using Newton's second law ($\sum F = m\ddot{u}$), and then approximate values for velocity and displacement using the mid-point rectangle approximation method.

4.2.1 Step-by-Step Iteration

Given the initial properties of the structure, we derive the equations of motion. Unlike in section 3.2, we only look at the free body diagram of the main structure alone for the first equation and get:

$$m\ddot{u} + c\dot{u} + ku - p - c_d\dot{u}_d - k_d u_d = 0 \tag{4.6}$$

$$m_d(\ddot{u} + \ddot{u}_d) + c_d\dot{u}_d + k_d u_d = 0 \tag{4.7}$$

Therefore we get the expression of acceleration for both masses:

$$\ddot{u} = \frac{p + c_d\dot{u}_d + k_d u_d - c\dot{u} - ku}{m} \tag{4.8}$$

$$\ddot{u}_d = \frac{-c_d\dot{u}_d - k_d u_d}{m_d} - \ddot{u} \tag{4.9}$$

Instead of calculating continuous values of the accelerations, we define a time-step Δt, and calculate a finite number of values of the accelerations, at each of these time steps. For any value of u (displacement, velocity or acceleration respectively), we define u_i as being the displacement, velocity, or acceleration respectively at time $i\Delta t$. Because we used MATLAB® [1] to implement such a code, and stored the values in matrices, the initial values were stored in step 1 (instead of step 0). Assuming we know the values at step i, the procedure to get values at step $i + 1$ is as follow:

1) Calculate the new values of acceleration:

$$\ddot{u}_{i+1} = \frac{p_i + c_d\dot{u}_{d,i} + k_d u_{d,i} - c\dot{u}_i - ku_i}{m} \tag{4.10}$$

$$\ddot{u}_{d,i+1} = \frac{-c_d\dot{u}_{d,i} - k_d u_{d,i}}{m_d} - \ddot{u}_{i+1} \tag{4.11}$$

2) Assume a linear evolution between $\ddot{u}_{i+1}$ and $\ddot{u}_i$, (as well as between $\ddot{u}_{d,i+1}$ and $\ddot{u}_{d,i}$)

3) Approximate the new values of $\dot{u}$, u, $\dot{u}_d$ and u_d at step $i + 1$ using the midpoint rectangle approximation method for integration, as illustrated in Figure 4.3.

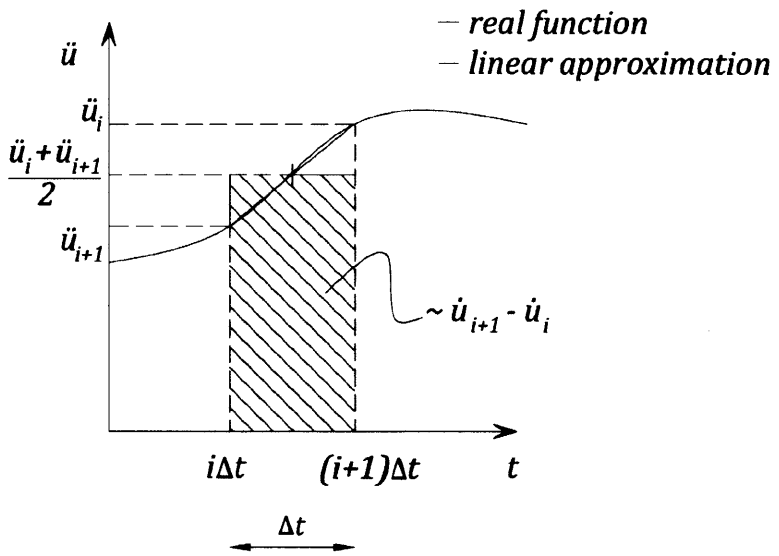

Figure 4.3: Approximation of Velocity

Velocities are therefore given by the equations:

$$\dot{u}_{i+1} = \dot{u}_i + (\frac{\ddot{u}_i + \ddot{u}_{i+1}}{2})\Delta t \tag{4.12}$$

$$\dot{u}_{d,i+1} = \dot{u}_{d,i} + (\frac{\ddot{u}_{d,i} + \ddot{u}_{d,i+1}}{2})\Delta t \tag{4.13}$$

Similarly, displacements are given by the equations:

$$u_{i+1} = u_i + (\frac{\dot{u}_i + \dot{u}_{i+1}}{2})\Delta t \tag{4.14}$$

$$u_{d,i+1} = u_{d,i} + (\frac{\dot{u}_{d,i} + \dot{u}_{d,i+1}}{2})\Delta t \tag{4.15}$$

Given the initial displacement and velocities values, we can compute each value of the displacement over a period of time t.

4.2.2 General Explanation of Code

The full code can be found in Appendix 2. This section describes what the code is doing, for ease of understanding.

In the first part of the code we define the properties of the structure (m, k, ξ, c). These were picked somewhat randomly, while trying to be as close as possible to real values found in actual buildings. The picked values are:

$m = 110{,}000{,}000\text{kg}$ (Weight of the ACT Tower, in Hamamatsu, according to Table 3.1)
$k = 35{,}300\text{N.m}^{-1}$ (Derivation is explained below)
$\xi = 2\%$ (Values in civil engineering range from 0 to 5%, in rare cases to 10%)
$c = 2m\xi\omega = 2m\xi\sqrt{\frac{k}{m}}$

To pick a value for k, we proceed as explained in section 4.1. As a first approximation, we assume that the building has the same stiffness κ for each floor; therefore, the stiffness matrix for the lumped mass system is a $n \times n$ size matrix, where n is the number of stories, and is given by:

$$\underline{K} = \begin{pmatrix} 2\kappa & -\kappa & & & & & \\ -\kappa & 2\kappa & -\kappa & & & 0 & \\ & -\kappa & 2\kappa & -\kappa & & & \\ & & \ddots & \ddots & \ddots & & \\ & & & -\kappa & 2\kappa & -\kappa & \\ & 0 & & & -\kappa & 2\kappa & -\kappa \\ & & & & & -\kappa & \kappa \end{pmatrix} \tag{4.16}$$

We assume that the worst case scenario happens for the first mode of the structure, which is a linear deformation. Therefore, the mode shape is given by:

$$\underline{\phi_1} = \frac{1}{n}\begin{bmatrix} 1 \\ 2 \\ \vdots \\ n-1 \\ n \end{bmatrix} \tag{4.17}$$

The 1 DOF system's stiffness is then given by:

$$k = \tilde{k}_i = \underline{\phi}_i^T \underline{K}\underline{\phi}_i = \frac{\kappa}{n} \tag{4.18}$$

Finally, we have to pick a value for κ, which we picked as a typical floor value according to the equivalent stiffness formula for fixed columns:

$$\kappa = f \frac{12\,EI}{h^3} \tag{4.19}$$

Where

$f = 19/6$ is a factor relating to the number of columns and their contribution.
$h = 4\text{m}$ is the height of a floor (typical value)
$EI = 15 \times 10^6 \text{N.m}^{-1}$ is the stiffness of one column (typical value)
$n = \frac{H_{total}}{h} = \frac{212}{4} = 53$ stories, where H_{total} has been picked as the ACT Tower height.

Using these values, we end up with:

$\kappa \approx 8{,}905{,}000\text{N.m}^{-1}$
$k \approx 168{,}000\text{N.m}^{-1}$

We then define the properties of the TMD. In real design, a damping ratio equivalent to the TMD's effectiveness can be derived. For engineers, this is the first value they are supposed to pick, according to displacement and acceleration constraints, and derive all of the TMD's properties from this value. However in this case, since we have no particular requirements, a random mass ratio will be chosen (still as close as possible to reality). Approximated formulas are then used [30] to calculate the optimal values for stiffness and damping, as follows:

$\bar{m} = 0.01$ (Mass ratio of 1%, usually varying between 0.05% and 2%)

$m_d = \bar{m}m$

$k_d = k\bar{m}\left(\frac{\sqrt{1-0.5\bar{m}}}{1+\bar{m}}\right)^2$ (Approximation of optimal stiffness for periodic excitation)

$\xi_d = \sqrt{\frac{\bar{m}(3-\sqrt{0.5\bar{m}})}{8(1+\bar{m})(1-0.5\bar{m})}}$ (Approximation of optimal damping ratio for periodic excitation)

$c_d = 2m_d\xi_d\omega_d = 2m_d\xi_d\sqrt{\frac{k_d}{m_d}}$

Values of the damper are optimized for periodic excitations only, which is not a problem, since wind produces periodic loading as have been discussed in Chapter 2.

Once structural properties are defined, we set up the time during which we will be viewing the response, as well as the time step interval (the shorter the time step, the better the approximation).

Matrices are created to store acceleration, velocity and displacement at each time step. We also give initial values which are required. We also create matrices to store acceleration, velocity and

displacement values of a system without a TMD, in order to compare results. A time matrix and a load matrix (which is the value of the load applied at each step) are created as well, and values are updated at each time step.

We then initialize the system with initial values for velocity and displacement, both for the structure and the TMD. The system without a TMD is initialized with the same values as the structure with the TMD. We then proceed to the step-by-step iteration described in section 4.2.1, which we also use to compute the displacement of the structure without the TMD – for the later, we use the same equations as the one with the structure, except we assume m_d, c_d and k_d to be equal to 0.

Finally we plot the results in different figures. The results are discussed below.

4.3 Simulation Results

4.3.1 Free Vibration

In the free vibration problem, the load matrix is constantly equal to 0, and initial values are given for displacements and velocity. Figure 4.4 shows the results for initial velocity and no initial displacement of the structure. Results only vary with a factor when adding initial displacement, or giving initial displacement without initial velocity.

Impulse functions make the system react similarly than for a free vibration problem. Therefore, they will not be discussed.

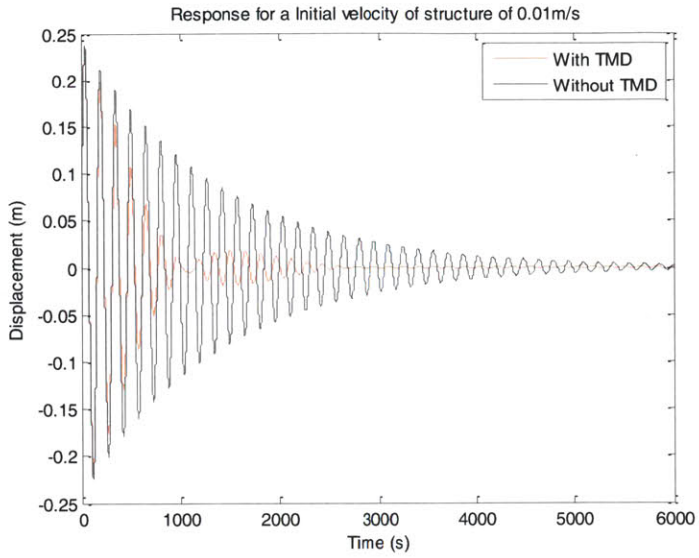

Figure 4.4: Free Vibration Response of a 1 DOF with Initial Velocity

Two things can be seen from the previous figure: first of all, the decay of movement is greatly increased with the addition of a TMD for free vibrations. The system takes 2500s to reach a steady state with a TMD versus 6000s without it, making the decay twice as fast with a TMD. Another interesting phenomenon can be seen for the structure with a TMD: after the structure has stopped moving (around 1000s), it restarts oscillating after a while.

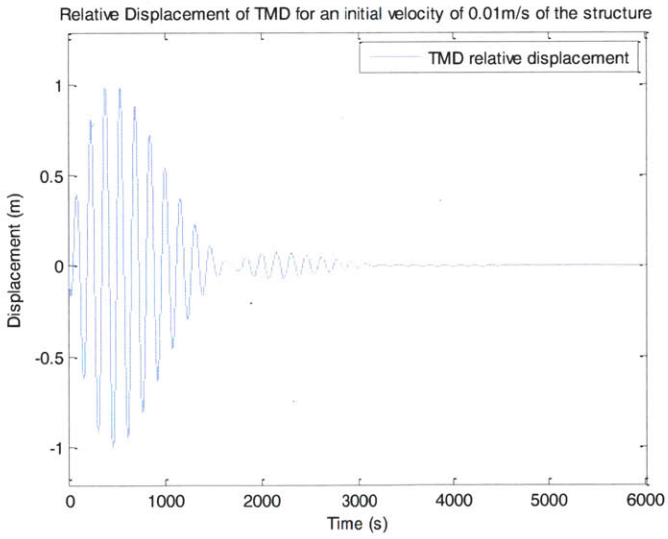

Figure 4.5: Relative Displacement of TMD Attached to a 1 DOF with Initial Velocity (Free Vibration)

Figure 4.5 shows the relative displacement of the TMD, and it can be seen that for 1000s, the TMD is still oscillating, thus creating a new force on the structure, which restarts oscillating. This can

be clearly seen in Figure 4.6, which compares the relative displacement of the TMD and the displacement of the structure. Figure 4.6 also shows that the TMD moves much more than the structure itself, which is one of the drawbacks we previously talked about.

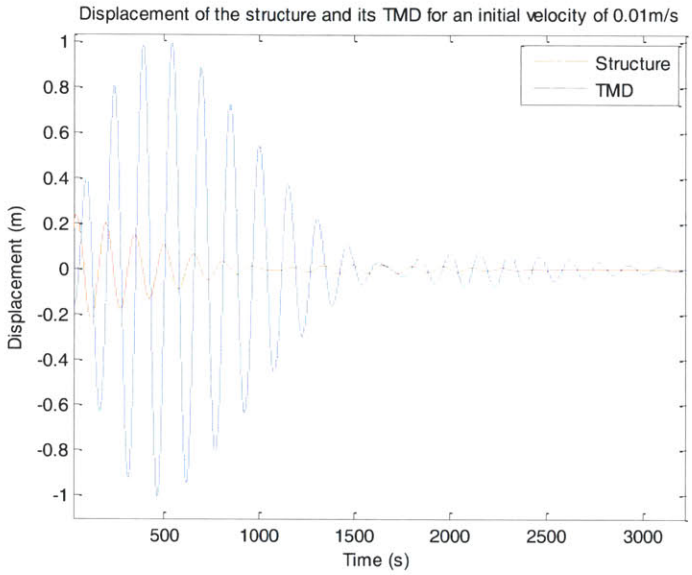

Figure 4.6: Displacement of Structure and its TMD for an Initial Velocity of 0.01m/s

4.3.2 Periodic Load

4.3.2.1 Harmonic Load

In this part, we apply a harmonic load to the structure. Several frequencies of harmonic loads are tried throughout this part. Applied loads are in the form of $p = 500\cos(\alpha \times \omega t)$, where ω is the natural frequency of the main structure, and α is a factor that will be varied. As can be predicted from Figure 4.7, the results with an optimal TMD should be:

- No different than without a TMD for $\alpha < 0.8$ or $1.15 < \alpha$
- Worse than without a TMD for $0.8 < \alpha < 0.96$ or $1.03 < \alpha < 1.15$
- Better than without a TMD for $0.96 < \alpha < 1.03$

This can be estimated by comparing the two continuous lines, which represent the amplification factor both for the optimally tuned case and the case without a TMD.

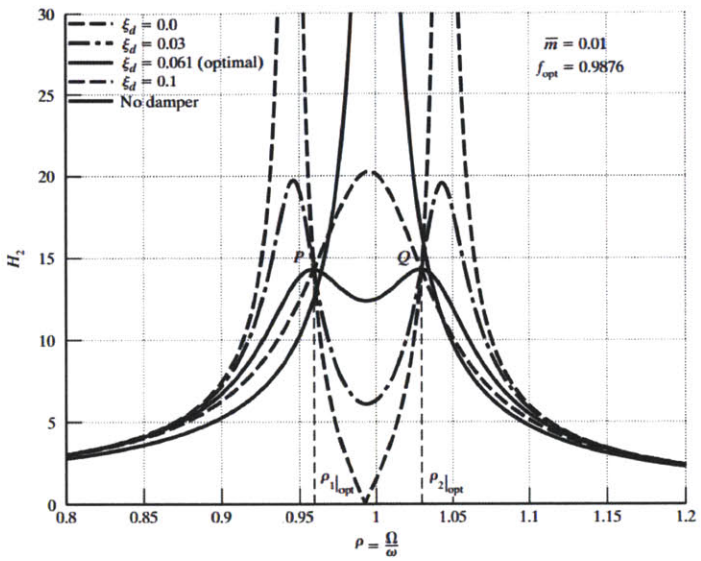

Figure 4.7: Response Curves for Amplitude of System with Optimally Tuned TMD [30]

4.3.2.1.1 No Effect

As predicted, for $\alpha < 0.8$ or $1.15 < \alpha$, there is no difference between the response of a structure with and without a TMD, in the steady-state, as is shown in Figure 4.8 ($\alpha = 0.2$). It is interesting, however, to notice that with a TMD, the structure reaches steady state faster.

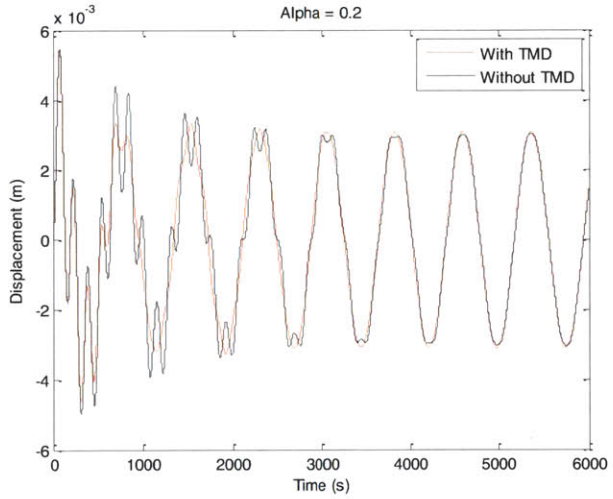

Figure 4.8: Non Effectiveness of the TMD for a Harmonic Load ($\alpha = 0.2$)

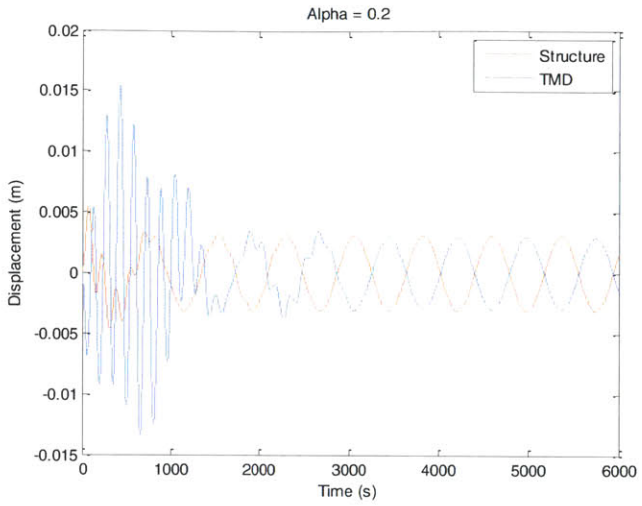

Figure 4.9: Response of a Structure and its TMD to a Harmonic Load ($\alpha = 0.2$)

Figure 4.9 shows that the TMD and the structure, unlike for free vibration, have the same order of magnitude during steady state. Furthermore, before the steady state, the TMD moves roughly 3 times more than the structure, whereas for free vibrations, the ratio was closer to 5 (Figure 4.6).

4.3.2.1.2 Worse Effect

For $0.8 < \alpha < 0.96$ or $1.03 < \alpha < 1.15$, the addition of a TMD should worsen the response of the structure. As an example, we pick the value of $\alpha = 0.92$.

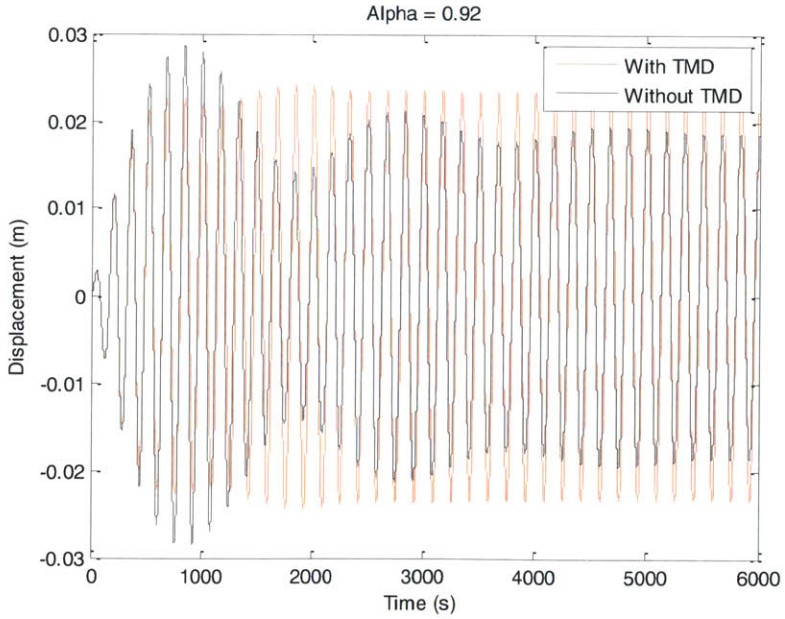

Figure 4.10: Worsening Effect of the TMD for a Harmonic Load ($\alpha = 0.92$)

Figure 4.10 compares the response of a structure with and without a TMD, for the worsening case. Although it is true that the TMD worsens the effect in the steady state response, the ratio is of 0.25/0.20, which is an increase by 25% of the response. Furthermore, the steady-state response is attained almost twice as fast with a TMD.

In terms of motion sickness, a TMD is less effective for such ranges of value of α. However, we can also see that the peak value without a TMD is 20% higher than the peak value with a TMD. Therefore, a TMD can be used in order to limit structural damage.

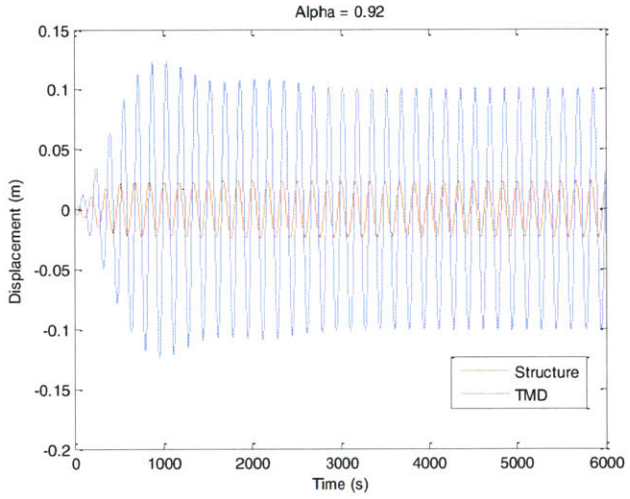

Figure 4.11: Response of a structure and its TMD to a harmonic load ($\alpha = 0.92$)

As seen in Figure 4.11, in this scenario, the TMD is once again moving 5 times more than the structure itself.

4.3.2.1.3 Beneficial Effect

For $0.96 < \alpha < 1.03$, the results of the effectiveness of the TMD are well observed. For this example, we picked a value of $\alpha = 0.997$. It can be seen that the response is almost divide by 4 when adding a TMD, which can be seen in Figure 4.12.

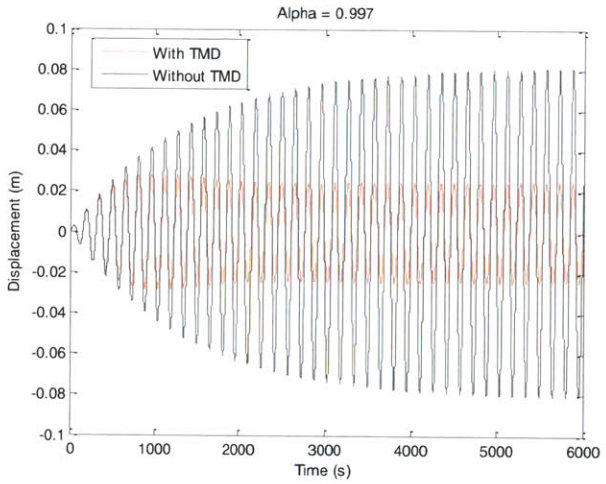

Figure 4.12: Beneficial Effect of the TMD for a Harmonic Load ($\alpha = 0.997$)

It is also interesting to note that the maximum amplitude of the response is roughly of 0.022m, which is the same value as in the worsening scenario (see Figure 4.10). Therefore, one of the main advantages of the addition of a TMD is the fact that the motion is controlled (in the sense that it stays even) for a wider range of frequencies than expected. (from 0.8 to 1.15, not only between 0.96 and 1.03).

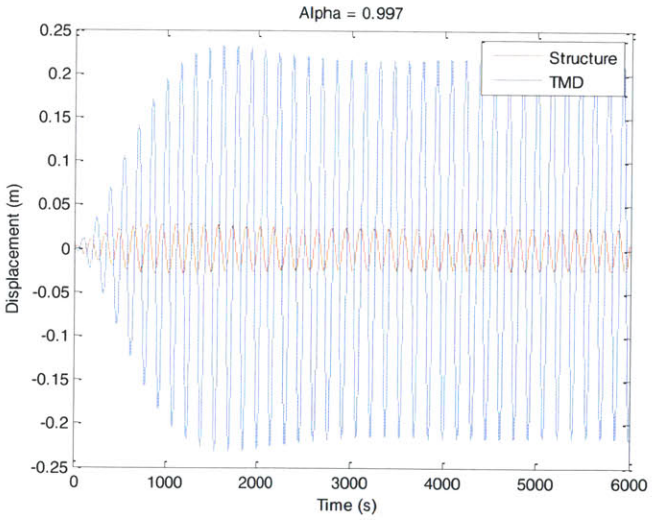

Figure 4.13: Response of a Structure and its TMD to a Harmonic Load ($\alpha = 0.997$)

Figure 4.13 shows the relative displacement of the TMD. Because it is "working" at full efficiency, the major drawback is that it moves drastically (more than 10 times the movement of the structure, with a displacement of ± 0.2m, which is equivalent to roughly ±8 inches).

All in all, although the TMD has positive and negative effects on the structure, we can say that its negative effects are relatively minor (25% increase in response) compared to its positive effect (75% decrease in response). Furthermore, the amplitude of movement of the structure is usually the same, whether the TMD has negative effects, or positive effects (0.02m), whereas they change drastically (from 0.02 to 0.08m) for a single DOF system without a TMD.

4.3.2.2 Saw Tooth Load

Although the harmonic load gives interesting results to the TMD, and its whole theory is based on harmonic excitation (see section 3.2), such an excitation is not always a good model of wind loads. It is a very good model for vortex shedding problems; however, we have to model loads in a different way if we want to understand the effects of along-winds on a structure.

As explained in Figure 2.3, wind is more of a saw tooth function, with random noise added to it. The period of wind is roughly of 2 to 3s. The following expression provides a good saw tooth function: $\frac{2}{\pi}\cos^{-1}(\cos(50\omega t)) - 1$, and is plotted in Figure 4.14.

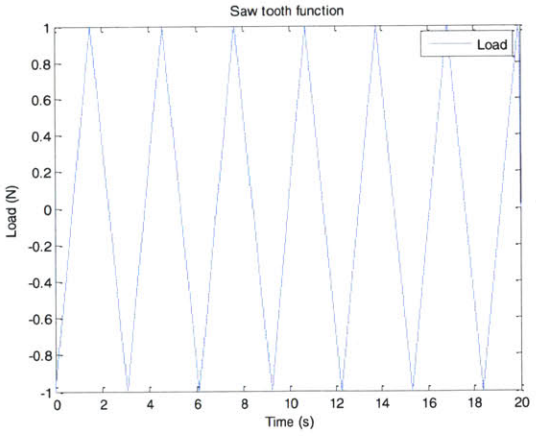

Figure 4.14: Saw Tooth Function

However, for some reason, the displacements of the structure are very hard to read (see Figure 4.15). This can either be due to bad approximations when calculating displacements (linear method of rectangles), or due to a bad model of the structure's properties (therefore, not reacting like a tall

building to 2 to 3s gusty winds). If the results are correct, this can also be representative of the vibrations the structure feels when subjected to gusty winds, which seems very unlikely.

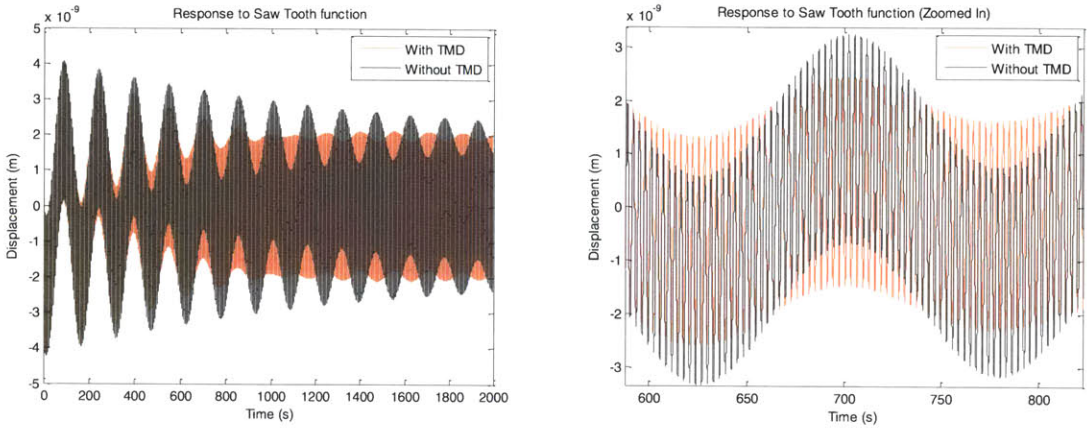

Figure 4.15: Response to Saw Tooth Function (Global and Zoomed In)

Gusty winds also have a random component, therefore, another exciting function can be applied, using the random function in MATLAB® [1]. The function is given as:

$$\frac{2}{\pi}0.1rand\ \cos^{-1}(\cos((50+0.5rand)\omega t))\ -\ 0.3rand - 1$$

and is plotted in Figure 4.16, with amplitude of 1. The *rand* function used here represents a random value between -1 and 1. The loading is much closer to the gusty load depicted earlier in Figure 2.3. Furthermore, for this type of loading, the response of the structure is clearer.

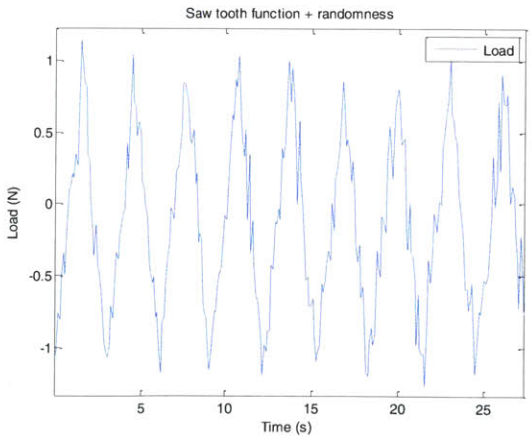

Figure 4.16: Random Saw Tooth Function

Examples of plot are shown in Figure 4.17. Overall, it is very hard to predict how the structure will react, but it can be seen that with the TMD, the structure has less ample oscillations, and they tend to decay very rapidly, which shows the effectiveness of TMDs.

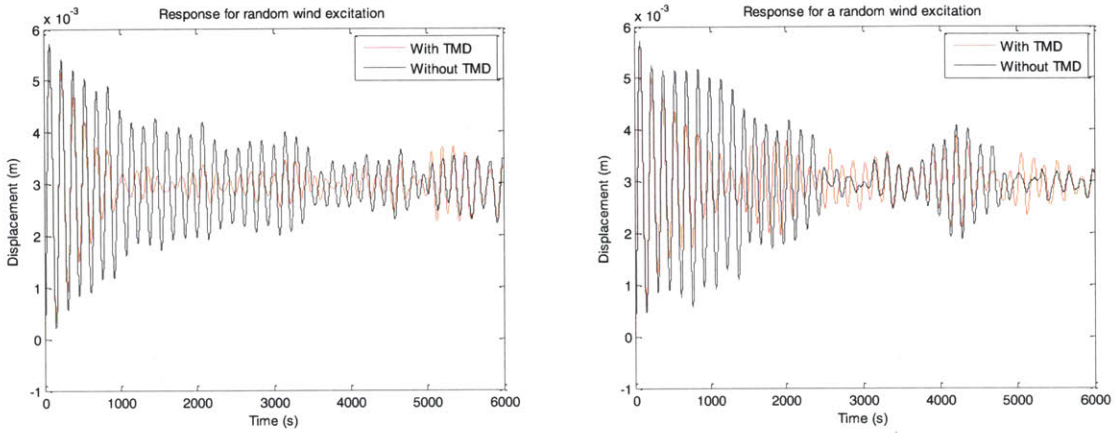

Figure 4.17: Response for Random Wind Type Loads

Similarly, Figure 4.18 shows the displacement of the TMD and the structure to the same random loads as Figure 4.17. In the same way the structure response is unpredictable, the TMD's movement cannot be foreseen because of the randomness involved. However, it is of interest to realize once again how the movement of the auxiliary system is much larger than that of the primary structure.

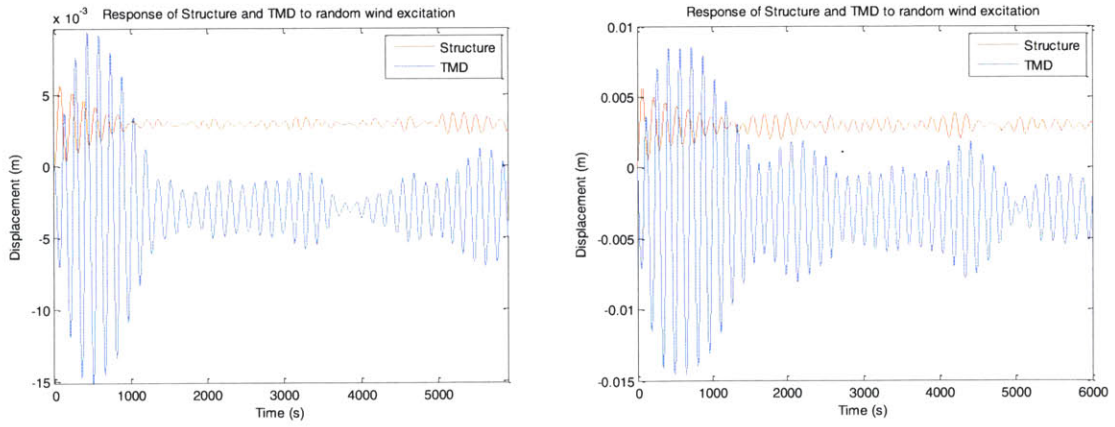

Figure 4.18: Response of TMD and Structure for Random Wind Type Loads

In terms of structure, it is interesting to note that one could expect the structure to react the same way with or without the TMD, as the saw tooth function is close to a harmonic excitation, with a

short period (i.e. a high frequency).Therefore, one could expect the solution to be the same as for $1.15 < \alpha$. However, it seems that because the loading is constantly changing, the system reacts as if it was subjected to multiple impulse functions. Further simulations show that an impulse function without any initial conditions will provide the same effect as a free vibration problem, in which we have shown that the TMD provides a beneficial effect on the structure. Therefore, the TMD reacts better because of the change in frequency of the loading. It seems, therefore, that the randomness of wind loading makes the TMD system work better.

With current trends in construction, one can only imagine that future construction will continue rising higher and higher. As this trend continues, we will more and more be faced with the challenge of mitigating motion, especially near the top of the buildings.

The Tuned Mass Damper proves to be a very effective solution to mitigate wind-induced vibrations in tall structures. However, one of the major drawbacks of such a device is its swaying around, which, according to simulations run, is fairly large. Nevertheless, the device gives very satisfactory results, both for harmonic excitations, which are a good representation of the vortex shedding problem, as well as for random saw tooth excitation, which are a better model for the gusty along-wind forces.

Several other forms of Tuned Mass Dampers have been developed in order to maximize the effect of the traditional spring mass damper, namely Tuned Liquid Columns, which provide flexibility in the form and no movement of the damper (only fluid moving in a tube), or semi-active dampers, which are capable of changing their properties to be effective on a wider scale of frequencies.

This study has not discussed all possibilities, and could be continued with more in-depth analysis. The code could be re-adapted in order to analyze response of a Tuned Liquid Damper (Sloshing or Column), or be used with varying stiffness and damping, in order to simulate the response of a Semi-Active Damper. Another possible pursuit of this topic would be to go into more precise models of building, in order to see the acceleration response of a full structure, as part of an analysis of motion sickness in buildings.

Table 1 Notation used in this Appendix

Notation	Meaning	Notation	Meaning	Notation	Meaning
AC	AC Servo Motor & Ball Screw	HR	Hallow Rubber Bearings	RS	Roller & Spring
AGS	Active Gyro Stabilizer	LB	Linear Bearing	S	Steel
AMD	Active Mass Damper	LCD (-PA)	Liquid Column Damper (with Period Adjusting Mechanism)	SLD	Sloshing Deep Water
C	Concrete	MP	Multiple Pendulum	SLS	Sloshing Shallow Water
CC	Circular	MR	Multiple Rubber Bearing	SRC	Steel and Reinforced Concrete
DD	Double Donut Type	HR	Hallow Rubber Bearings	TMD	Tuned Mass Damper
ξ	Damping Ratio (percent critical)	OD	Oil Damper	UT	U-Tube
EQ	Earthquake	PE	Pendulum	VD	Viscous Damper
HA	Hydraulic Actuator	R	Response	VED	Visco-elastic Damper
HMD	Hybrid Mass Damper	RC	Rectangular	W	Wind

Table 2 Applications of inertial type dampers

No	Building	Structure/ Use	Year	No. of Stories Height/ Area[m/m²]	Building Weight generalized [t]	Period (x, y, tor) [s]	Equipment/ Mechanism*	Mass of Damper [t]	Mass Ratio (Generalized)	Max Stroke/ Actuator Specs	Intended Application/ Performance
· 1	ACT Tower, Hamamatsu	S/Office, Hotel	1994	+45.-2 212.0/ 151000	110000	4.52 4.73	TMD(x), HMD(y) MP/OE	90×2 (x, y)	0.16%	±90 cm (x) ±150 cm (y)	W, ξ=0.9%(ξ); ΔP=10% (ψ)
· 2	Akita Tower, Akita	S/Tower	1994	-- 112.1/ 4773	2186 (1012)	2.30 2.30	TMD/MR/OE	15 15	0.69% 0.69%	±60 cm	EQ/W
· 3	Ando Nishikicho Bldg., Tokyo	S/Office	1993	+14. -2 68/ 4928.3	2600	1.47 1.39 --	HMD/HMD HR AC	20 (TMD)+ 2(AMD) ×2	0.85%	TMD ±15cm AMD ±50 cm	EQ/W, ξ=+6.4%, +8.5% (ξ, ψ); P=-69% (ξ), -52%(ψ)
· 4	Building M, Osaka	S/ Residence, Office	1994	+9 30.4/345		0.75 0.65	TMD (2 dir) MR	2.44 +0.79	0.9%	2.6 cm	W R=-33%
· 5	Building S, Osaka	S/Office	1994	+9 30.9/--		0.59, 0.78, 0.55	TMD	1.0 (y) 1.75 (torsion)			ξ=+2.4% (y); +2.7% (torsion)
· 6	Chiba Port Tower, Chiba	S/Tower	1986	-- 125/2308	1950 (1200)	2.25 2.70	TMD/RS/VD	10.0 15.6	0.51% 0.80%	±100 cm	EQ/W R=55% (20 m/s)
· 7	Chifley Tower, Sydney	S/Office	1994	-- 209/--			TMD/PE	400	2%	±910 mm	W ξ=2-4%
· 8	Citicorp Building, New York	S/Office	1978	-- 278/--			TMD	410 bi-axial		2.18 m	W R=45-50%
· 9	CN Tower, Toronto	S/C/Tower	1975	-- 553/--			TMD/PE	20			W
· 10	Complex Building in Shinjuku	S/Complex		+36, -4 150/ 80000			AMD, Gear PD Linear Motor	30×2		±1 m	
· 11	Crystal Tower, Osaka	S/Office	1990	+37.-2 157/ 85994	44000	3.60 4.10	TMD (Ice Thermal Tank) PE, OE	180 (x) 360 (y)	0.41% 0.82%	±25 cm	W R=1/2
· 12	Dowa Kasai Phoenix Building, Osaka	S/Office	1994	+29. -3 145.4 30,370	27000	2.80 2.88 2.17	HMD/HMD HR AC	30 (TMD)+ 6x2 (AMD)		TMD: ±50 cm, AMD: ±100 cm	W/EQ, W R=-45%(x), -60%(y)
· 13	Elevator Tech. Lab., Tokyo	S/ Exp. Tower	1992	-- 60.0/630			AGS				W
· 14	Experimental Tower	S/Tower	1993	6 18.3	154.4	1.06 1.11 --	Active Fin 2 m×1 m, 0.1 m thick, AC				
· 15	Experimental Elevator Building	S/Tower	1997	-- 145	6877	2.86 2.44	HMD	34.5 (x) 26.8 (y)	1.73% (x) 1.41% (y)	±40 cm (x) ±40 cm (y)	W R=-1/3 ξ=+8-11%
· 16	Fujita Experimental Building	RC/Base Isolation System	1995	3 10		0.8 0.8 --	HMD AC	4.13 4.34	(1.3%)		ξ=+11%
· 17	Fukuoka Tower, Fukuoka	S/Tower	1989	-- 150.7/ 1808	4000	3.30 3.20	TMD/RS/ OE	30 25	0.75% 0.63%	C±110 cm	EQ/W
· 18	Gold Tower, Kagawa	S/Tower	1988	-- 144/ 1193		2.69 2.50	TLD/SLD/RC 45×250×10 0-16 (53 cm)	9.6			W R=1/2~1/3

Table 2 Continued-I

No	Building	Structure/ Use	Year	No. of Stories Height/ Area[m/m²]	Building Weight generalized [t]	Period (x, y, tor) [s]	Equipment/ Mechanism*	Mass of Damper [t]	Mass Ratio (Generalized)	Max Stroke/ Actuator Specs	Intended Application/ Performance
· 19	John Hancock, Boston	S/Office	1977	-- 243.84/--			TMD	2×300 uniaxial			W R=40-50%
· 20	Hankyu Chayamachi Bldg. (Applause Tower), Osaka	S/Office, Hotel	1992	+34 -3 161/89686	13943	4.7 4.8 --	AMD/AMD (Helideck) MR HA	480 (x, y)	(x: 3.4%) (y: 3.9%)	5t×2×2 ±30cm	W ξ=+9.2%
· 21	Herbis Osaka, Osaka	S/Office, Hotel	1997	+40 -5 190/--	22749	5.1 5.4 5.5	AMD (Heat Storage Tanks)	2×160	1.41%	±30 cm 5t×2	W
· 22	Hibikiryokuchi Sky Tower, Kitakyushu	S/ Observatory	1991	-- 135/--			TMD				
· 23	Higashiyama Sky Tower, Nagoya	S/Tower	1989	-- 134/2929	(1870) (1960)	2.20 1.98	TMD/PE/OE	19.8 (x, y)		±15 cm	W
· 24	High-rise Housing Exp. Tower	S/Truss Tower	1995	-- 108/--	730		AGS	Flywheel 0.8×2	(0.7%)		W R=-50%
· 25	Hirobe Miyake Bldg., Tokyo	S/Office, Residential	1994	+9 30.65/--	273	0.63 0.81 0.48	HMD HR AC	2.11 -	(1.7%)	0.806t 2.2kW ±30 cm	W ξ=+14.4% R=-66%
· 26	Hobart Tower, Tasmania	S/Tower		-- 105/--			80 SLS				
· 27	Hotel COSIMA, Tokyo	S/Hotel	1994	+26 -3 106.35/9798	4600 (1160)	2.0 2.1	LCD-PA UT 600 x150x290 -4	58	1.3%	±72 cm	W R=-40%
· 28	Hotel Ocean 45, Miyazaki	S/Hotel	1994	+43. -2 154.3	83,650	3.6 3.9	HMD (x) TMD (y) MR AC	120×2 (x, y)	0.29%	±50 cm (y) ±100 cm (x)	W R=-35%
· 29	Huis Ten Bosch Tower, Nagasaki	S/Tower	1992	-- 105.0/--	4599	1.75 1.75	TMD/MR/ VED	7.8	0.17%	±80 cm	W R=1/2~1/3
· 30	Hyatt Hotel, Osaka	S/Hotel	1995	28 112/--	43000		LCD-PA	104	(0.24%)		W R=-30%
· 31	KS Project, Kanazawa	S/--	1993	-- 121/--			AMD				
· 32	Kansai New Airport Tower, Osaka	S/Tower	1994	-- 86/--	2570	1.25 1.25	HMD/HMD PE, AC	5×2 (x, y)	0.19%	7.5kW×2 ±30 cm	W R=-50% ξ=5~7%
· 33	Kyobashi Seiwa Bldg., Tokyo	S/Office	1989	+11.-1 32.8/423	340	1.1 1.5 1.9	2 AMD PE HA	4.0 1.0	1.5%	1t, 0.25t, 22 kW, ±25 cm	EQ/W R=1/3 (23 m/s)
· 34	Landmark Tower, Yokohama	S+SRC/ Office, Hotel	1993	+70 -3 296/231060	261000 (50000)	5.1 5.1 3.6	HMD/HMD MP, AC	170×2 (x, y)	(0.68%)	30t×2×2 60kW×2 ±170 cm	W R:-48% ξ=+10%
· 35	L.T.C. Bank of Japan Bldg., Tokyo	S/Office	1993	+21. -5 130.0/62821	39800 (30,400)	2.4 2.6	HMD (Heat Storage Tanks) MR HA	195 (x, y)	(0.65%)	30t×2×2 60kW×2 ±100 cm	EQ/W ξ=+6.3~14.3% W R=-30% EQ R=-50%
· 36	MHI Yokohama Bldg., Yokohama	S/Office	1994	+34 -2 151.9/ 110918	61800	3.9 3.8	HMD (2 dir) PE	80 (PD=60)	0.13%	0.8 m	W

Table 2 Continued-II

No	Building	Structure/ Use	Year	No. of Stories Height/ Area[m/m²]	Building Weight generalized [t]	Period (x, y, tor) [s]	Equipment/ Mechanism*	Mass of Damper [t]	Mass Ratio (Generalized)	Max Stroke/ Actuator Specs	Intended Application/ Performance
·37	MHS Design Office, Tokyo	S/Office	1988	+8.-1 26.8/940		0.7	TMD/PE/OE	2.5×2			EQ/W
·38	MKD8 Hikarigaoka, Tokyo	S/Office, Hotel	1993	+24. -3 100/--	29000 (9200)	2.0 1.7	HMD/HMD PE, AC	22×2 (x, y)	(0.47%)	15kW×2×2 x: ±25 cm y: ±40 cm	W ξ=+6% R=-30%
·39	NTT CRED Motomachi Bldg., Hiroshima	S/Hotel, Office	1993	+35 -2 150/ 170000	83000	3.8 3.6	HMD (1 dir) PE	110 (PD=80)	0.13%	0.6 m	W
·40	Nagasaki Airport Tower, Nagasaki	S/Tower	1987	-- 42.0/--	170	0.93 0.93	TLD/SLS/CC 38 φ×7-175 (4.8 cm)	0.95	0.56% (1.5%)		W R=35% (20 m/s)
·41	Nanjing TV Tower, Nanjing, China	C/Tower	1999	-- 340/--	-- (2431)	5.05	AMD	~60	1%	1.5 m 50 kN	
·42	Narita Airport Tower, Chiba	S/Tower	1993	-- 87.3/--	4140	0.78 0.75 0.48	TLD/SLS/CC 50 φ×12.5-2310 (3.64 cm)	16.5	0.40%		W
·43	O Building, Nagasaki	S/Office	1990	-- 27/--			TLD				
·44	Ohita Prefecture Cultural Hall	S+SRC/ Office & Convention	1998	+21 -3 101 m 83,297	20,000		HMD (Linear Motor)	25×2	0.25%	±800 cm	Active: W R=1/3 (26 m/s) Passive: W R=1/2 (50 m/s)
·45	ORC 200 Symbol Tower, Osaka	S/Office, Hotel	1992	+50. -3 200/ 72097	56680 (15600)	4.72 4.4 --	TMD (x) HMD (y)/ MR/VED	115×2 (x, y)	0.41% (1.47%)	x: ±50 cm y: ±100 cm	W R=50%
·46	Osaka World Trade Center Building., Osaka	S/Office	1994	+52. -3 252.0/ 147000	75000	5.84 5.84	HMD/HMD MP AC	50×2 50×2		75t×2×2 37kW× 2×2 ±160 cm	W
·47	Pipe Lab., Kanagawa	S/ Experimental Tower	1990	+12 33.8/300		2.09	TLD/SLS	1.1			EQ
·48	Plaza Ichihara, Chiba		1995	+12 61/--	5760		HMD	14	0.24%		
·49	Porte Kanazawa, Kanazawa	S/Hotel, Office	1993	+30 -2 131/--	10150	2.9 (x) 2.5 (tor)	HMD MR AC	50×2	(0.49%)	5 t×2 ±15 cm	ξ=+2% (x) +5.5% (tor)
·50	Rinku Gate Tower Bldg, Osaka	S/Hotel	1995	+56 -2 254/--	75000	4.4 4.4	HMD MP AC				
·51	Riverside Sumida Building, Tokyo	S/Office, Residential	1994	+33. -2 134.4/ 60000	52000	-- 2.86 2.32	AMD (y) LB AC	15×2	(0.058%)	8.7t×1×2 55kW× 1×2 ±100 cm	EQ/W D=+7.1%(y) EQ R= -20~30%
·52	Rokko-Island P&G, Kobe	S/Office	1993	+31. -1 131/46076	27000	1.64 2.94 1.69	TMD (Ice Thermal Tank) PE/OE	y: 90×2 torsion: 90	1.0%		W ξ=y: +5.4% R=-60%
·53	Sea Hawk Hotel, Fukuoka	S/Hotel	1995	36 143/--	42000		TMD (Water Tank) PE	112~132	(2-2.5%)		W ξ=+3.6% R=-50%
·54	Sendagaya INTES Bldg., Tokyo	S/Office	1991	+11. -1 58.0/10602	3280	-- 1.7 2.1	AMD/AMD PE HA	36×2 (y)	(2.2%)	5t×1×2± 15 cm	EQ/W WR=-18% (y) WR=-28% (tors) ξ=+8%

Table 2 Continued-III

No	Building	Structure/ Use	Year	No. of Stories Height/ Area[m/m²]	Building Weight generalized [t]	Period (x, y, tor) [s]	Equipment/ Mechanism*	Mass of Damper [t]	Mass Ratio (Generalized)	Max Stroke/ Actuator Specs	Intended Application/ Performance
· 55	Sendai AERU	SRC Multi-purpose	1998	+33 -3 145.5/ 73,131			TMD Laminated Rubber+ Coil Spring	100 (6.7 m × 7.2 m × 3.4 m, two ways each) × 2	0.7%		W R=1/2
· 56	Shanghai World Financial Center	S+RC/Office, Hotel	2001 (?)	+94 -3 460/ 333600			SLS, ϕ 7.5 m	8 × 100 t			W
· 57	Shimizu Corp. Tech. Lab., Tokyo	S/ Experimental Tower	1991	+7. -1 30.0/-	400	0.88 1.05	HMD/AMD MR AC	4.95 (x, y)	(1.2%)	1.2t × 2 7.5kW × 2 ±23 cm	EQ/W ξ=20%(15 m/s)
· 58	Shin-Yokohama Prince Hotel, Yokohama	S/Hotel	1991	+42. -3 149.3/ 76027	26400 (10500)	4.43	TLD/SLS/ CC 200 ϕ × 20.5-270 (9.85 cm)	101.7	0.39%		W R=1/2 (20 m/s)
· 59	Shinjuku Park Tower, Tokyo	S/ OfficeHotel	1994	+52. -5 226.5/ 264100	130000	4.5 5.24 3.98	HMD (y) VR AC	110 × 3 (y)	(0.25%)	75kW × 1 × 3 ±100 cm	W D=+4% R=~50%
· 60	Sydney Tower, Sydney	S/Tower	1981	305/--			TMD/PE	180 40		±150 mm	W R=-40-50%
· 61	T Building	S/Office	1997	9 31.1/--	842	0.81 0.66	TMD PE	8.5	1%		W: R=-50% ξ=+5.6%
· 62	TYG Building, Atsugi	--/Office	1992	-- 58.6/--	7450	1.89	TLD (DD) D1=68.6 cm d1=48.6 cm D2=42 cm d2=29.5 cm	18.2	0.24	N/A	W
· 63	Takenaka Corp. Tech. Lab, Tokyo	S/Exp. Tower	1989	+7 22.8/--		1.11 1.54	AMD/AMD PE HA	6.0 (x,y)		10t × 2 ±95 cm	EQ/W
· 64	Toda Corp. Tech. Lab., Tokyo	S/Exp. Tower	1992	+6 18.9/--		1.33 1.13	HMD/HMD LB HA	5.5 4.11	1.0%	1t × 2, 11 kW, 5 cm	EQ/W: R=1/3~1/4 ξ=2~5%
· 65	Tokyo International Airport Tower, Haneda	S/Tower	1993	-- 77.6/--	3240	1.3 1.0	TLD/SLS/ CC 60 ϕ 12.5-1404 (5.3 cm)	22.7	0.70%		W R=1/2 (20 m/s) R=2/3 (20 m/s)
· 66	Washington National Airport Tower, USA	S/Tower	1997	-- 67.5/--		1.42 1.52	TMD	20 kips			W ξ=+3%
· 67	Yokohama Marine Tower, Yokohama	S/Tower	1987	-- 101.3/3326	540	1.82	TLD/SLS/ CC 50 ϕ × 5-390 (2.2. cm)	1.54	0.29%		W R=1/3 (20 m/s)
· 68	Yoyogi 3-Chrome Kyodo Building	S+SRC School	1998	+20, -2 89 56,300			TMD (x)+ HMD (y) AC Servo	40 (4.7 m × 4.7 m × 2.4 m, two ways each) × 2	0.1%		W: 1/2

*for TLD: container dimensions-no. of units (level of liquid in unit)

(Communicated by Managing Editor)

```
%Draws timehistory of movement of a 1 DoF System.

%Define Structure properties

m = 100000000;      % Weight of structure (kgs)
k = 168000;         % Stiffness of structure (N.m-1)
w = sqrt(k/m);      % Natural frequency of structure
ksi = 0.02;         % Damping ratio of structure
c = 2*m*ksi*w;      % Damping of structure (N.s.m-1)

%Define Optimal properties for TMD

mbar = 0.01;                                                        % Mass ratio
md = mbar*m;                                                        % Mass of TMD (kgs)
kd = k*mbar*(sqrt(1-0.5*mbar)/(1+mbar))^2;                          % Optimal stiffness of TMD (N.m-1)
wd = sqrt(kd/md);                                                   % Natural frequency of TMD
ksid = sqrt((mbar*(3-sqrt(0.5*mbar)))/(8*(1+mbar)*(1-0.5*mbar)));   % Optimal damping ratio of TMD
cd = 2*md*ksid*wd;                                                  % Optimal damping of TMD (N.s.m-1)


% Define time properties

tmax = 6000;        % Length of time during which the respons will be analyzed
dt = 0.1;           % Time step interval
n = floor(tmax/dt); % Number of steps

% Create matrices in which to store aceleration, velocity, displacement and time

    % For the structure
    a = zeros (n+1,1);  % Structure's acceleration
    v = zeros (n+1,1);  % Structure's velocity
    x = zeros (n+1,1);  % Structure's displacement

    % For the TMD
    ad = zeros (n+1,1); % TMD's acceleration
    vd = zeros (n+1,1); % TMD's velocity
    xd = zeros (n+1,1); % TMD's displacement

    % For the structure without the TMD
    A = zeros (n+1,1);  % Structure without TMD's acceleration
    V = zeros (n+1,1);  % Structure without TMD's velocity
    X = zeros (n+1,1);  % Structure without TMD's displacement

    % For Time
    t = zeros (n+1,1);  % Time matrix

    % For the load
    p = zeros (n+1,1);  % Load matrix

% Define initial conditions (Initial velocity and displacement)

    % For Structure
    v(1) = 0;   % Initial velocity
    x(1) = 0;   % Initial displacement

    % For TMD
    vd(1) = 0;  % Initial velocity
    xd(1) = 0;  % Initial displacement

    % For Structure without TMD, which should be identical to those of the Structure WITH the TMD
    V(1) = v(1);% Initial velocity
    X(1) = x(1);% Initial displacement
```

```
63
64      % Define, when required, an initial load
65      p(1) = 0;
66
67  % Start the step-by-step implementation
68
69  for i=1:n
70
71      t(i+1)= i*dt;                   % Fill up the Time Matrix as we loop
72
73      p(i) =  500*cos(0.95*w*t(i));   % Define the load at step i
74
75      % Derive acceleration, velocity and displacement of the structure
76
77      a(i+1)=(p(i)+cd*vd(i)+kd*xd(i)-c*v(i)-k*x(i))/m;        % See Equation (4.10)
78      v(i+1)=v(i)+(a(i)+a(i+1))/2*dt;                         % See Equation (4.12)
79      x(i+1)=x(i)+(v(i)+v(i+1))/2*dt;                         % See Equation (4.14)
80
81      % Derive acceleration, velocity and displacement of the TMD
82
83      ad(i+1)=(-cd*vd(i)-kd*xd(i))/md - a(i+1);               % See Equation (4.11)
84      vd(i+1)=vd(i)+(ad(i)+ad(i+1))/2*dt;                     % See Equation (4.13)
85      xd(i+1)=xd(i)+(vd(i)+vd(i+1))/2*dt;                     % See Equation (4.15)
86
87      %acceleration, velocity and displacement of the structure without TMD
88
89      A(i+1)=(p(i)-c*V(i)-k*X(i))/m;                          % Same as Equation (4.10), where kd=cd=0
90      V(i+1)=V(i)+(A(i)+A(i+1))/2*dt;                         % See Equation (4.12)
91      X(i+1)=X(i)+(V(i)+V(i+1))/2*dt;                         % See Equation (4.14)
92
93  end
94
95  % Plot the results
96
97  figure();                                   % Create a new figure on which to plot the results
98  plot(t,x,'r');                              % Plot the displacement of structure with TMD in red
99  hold on;                                    % Hold, to keep all the results on the same plot
100 plot(t,X,':k')                              % Plot the response without the TMD in black dots
101 legend('With TMD', 'Without TMD');          % Label the Figure
102 xlabel('Time (s)');                         % Label X axis
103 ylabel('Displacement (m)');                 % Label Y Axis
104
105
106 figure();                                   % Create a new figure on which to plot the results
107 plot(t,x,'r');                              % Plot the displacement of structure with TMD in red
108 hold on;                                    % Hold, to keep all the results on the same plot
109 plot(t,xd-x,'b')                            % Plot the relative displacement of TMD in blue
110 legend('Structure', 'TMD');                 % Label the Figure
111 xlabel('Time (s)');                         % Label X axis
112 ylabel('Displacement (m)');                 % Label Y Axis
113 hold off;                                   % Hold off, for later simulations
```

[1] MATLAB version 7.13.0.564. Natick, Massachusetts: The MathWorks Inc., R2011b.

[2] "SkyscraperPage.com." *SkyscraperPage.com*. Ed. Skyscraper Source Media. Web. 12 Apr. 2012. <http://www.skyscraperpage.com/>.

[3] "Pyramides D'Egypte." *Wikipedia*. Wikimedia Foundation, 01 Apr. 2012. Web. 12 Apr. 2012. <http://fr.wikipedia.org/wiki/Pyramides_d'Egypte>.

[4] "History of Structural Analysis." Web blog post. *Engineer's Outlook*. Ed. Engineer's Outlook. WordPress.com, 12 Jan. 2012. Web. 12 Apr. 2012. <http://engineersoutlook.wordpress.com/2012/01/12/history-of-structural-analysis/>

[5] Atsushi, Ueda. "Five-story Pagodas: Why Can't Earthquakes Knock Them Down? Wisdom from the Distant Past." *NIPPONIA*. Web Japan, 15 June 2005. Web. 12 Apr. 2012. <http://web-japan.org/nipponia/nipponia33/en/topic/index.html>.

[6] Iliff, David. Washington Monument, Washington D.C. Digital image. *Wikipedia*. 12 Jan. 2006. Web. 13 Apr. 2012. <http://en.wikipedia.org/wiki/Washington_Monument>.

[7] Lieu Song, Benh. Tour Eiffel. Digital image. *Wikipedia*. 1 June 2009. Web. 13 Apr. 2012. <http://en.wikipedia.org/wiki/Eiffel_Tower>.

[8] Barss, Karen. "The History of Skyscrapers - A Race to the Top." *Infoplease.com*. Infoplease.© 2000–2007 Pearson Education, publishing as Infoplease. Web. 14 Apr. 2012 <http://www.infoplease.com/spot/skyscraperhistory.html>.

[9] Council of Tall Building and Urban Habitat. "CTBUH Skyscraper Center." *Skyscraper Center*. Web. 17 Apr. 2012. <http://skyscrapercenter.com/>.

[10] Reina, Peter. "Megastructure Supports Taipei's 508-Meter 'Megatower'." *Engineering News-Record*. 24 Nov. 2003. Web. 3 May 2012. <http://enr.construction.com/projects/international/archives/031124a.asp>.

[11] Taipei Financial Center Corp. "TAIPEI 101 Observatory." *TAIPEI 101*. 2009. Web. 03 May 2012. <http://www.taipei-101.com.tw/en/DB/index.asp?id=db01>.

[12] Probyte2u. "Taipei 101 - Tuned Mass Wind Damper." *HubPages*. Web. 08 May 2012. <http://probyte2u.hubpages.com/hub/Taipe1-101-Tuned-Mass-Wind-Damper>.

[13] "SWFC's Superlative Structure." *Shanghai World Financial Center*. Mar. 2011. Web. 29 Apr. 2012. <http://www.swfc-shanghai.com/about/press/newsletter/en/201103.html>.

[14] *SWFC - Active Tuned Mass Damper. Youtube*. Mori Building, 20 June 2007. Web. 29 Apr. 2012. <http://www.youtube.com/watch?v=BK-sAqBUwxk>.

|15] Taranath, Bungale S. "Chapter 5. Wind Loads." *Structural Analysis and Design of Tall Buildings: Steel and Composite Construction*. Boca Raton: CRC/Taylor & Francis, 2011. Print.

[16] Mendis, P., T. Ngo, N. Haritos, A. Hira, B. Samali, and J. Cheung. *Wind Loading on Tall Buildings*. Electronic Journal of Structural Engineering, 2007. Special Issue: Loading on Structures, p. 41-54. *Instituto Nacional De Tecnologia Industrial*. Web. 22 Apr. 2012. <http://www.inti.gov.ar/cirsoc/pdf/accion_viento/200704.pdf>.

[17] Wargon, Alex, and Andrew Davids. "Wind Resisting Structural Systems for Tall Buildings." *Tall Buildings: 2000 and Beyond*. Bethlehem, PA: Council on Tall Buildings and Urban Habitat, 1990. p. 257-71. Print.

[18] Irwin, Peter A. "Exposure Categories and Transitions for Design Wind Loads." *Journal of Structural Engineering* 132.11 (Nov. 2006). *ASCE Library*. American Society of Civil Engineers. Web. 24 Apr. 2012. <http://ascelibrary.org/sto/resource/1/jsendh/v132/i11/p1755_s1?view=fulltext>.

[19] Schueller, Wolfgang. *High-Rise Building Structures*. New York: John Wiley & Sons, 1977. Print.

[20] Kilpatrick, John. *The Influence of Wind-Induced Motions on the Performance of Tall Buildings*. Thesis. University of Western Ontario, 1996. *Library and Archives Canada*. National Library of Canada. Web. 24 Apr. 2012. <http://www.collectionscanada.gc.ca/obj/s4/f2/dsk2/ftp04/MQ39839.pdf>.

[21] McCauley, Michael E., Jackson W. Royal, C. Dennis Wylie, James F. O'Hanlon, and Robert R. Mackie. *Motion sickness incidence: exploratory studies of habituation, pitch and roll, and the refinement of a mathematical model*. Human Factors Research Inc. Technical Report 1733-2, 1976.

[22] Chang, Fu-Kuai. *Wind and movement in tall buildings*. ASCE Civil Engineering, Vol. 37, NO. 8, 1967, p. 70-72

|23] Chen, Peter W. and Leslie E. Robertson. *Human perception thresholds of horizontal motion*. Journal of the Structural Division. Proceedings of the ASCE, Vol. 98, No. ST8, August, 1972, pp.1681-1696

[24] Hansen, Robert J., John W. Reed, and Erik H. Vanmarcke. *Human Response to Wind-Induced Motion of Buildings*. Professional Paper No. P72-6. Structures Publication No. 356. Cambridge: Massachusetts Institute of Technology, October 1972. Print.

[25] Council on Tall Buildings and Urban Habitat. *Motion Perception and Tolerance*, Chapter PC-13, Vol. PC of Monograph on Planning and Design of Tall Buildings, ASCE, New York, 1981.

[26] Halvorson, R. A. and Nick Isyumov. *Dynamic response of Allied Bank during Alicia*. Proceedings of Special Conference "Hurricane Alicia-One Year Later", Aerospace Division, Structural Division, ASCE, Galveston, Texas, August 16- 17, 1984.

[27] Kanda, Jun, Yukio Tamura, Kunio Fujii, Tamio Ohtsuki, Kiyoto Shioya and Shinji Nakata. *Probabilistic evaluation of human perception threshold of horizontal vibration of buildings*. Proc. ASCE Structures Congress 95, Boston, Ma., 1995.

[28] Tamura, Yukio, Seizo Kawana, Osamu Nakamura, Jun Kanda, and Shinji Nakata. *Evaluation Perception of Wind-induced Vibration in Buildings*. Proceedings of the ICE - Structures and Buildings Vol. 159. Issue 5. 1 Oct. 2006. Web. 18 Apr. 2012.
<http://www.icevirtuallibrary.com/content/article/10.1680/stbu.2006.159.5.283>.

[29] Isyumov, Nick. *Criteria for acceptable wind-induced motions of tall buildings*. International Conference on Tall Buildings, Council on Tall Buildings and Urban Habitat, Rio de Janeiro, May 17-19, 1993.

[30] Connor, Jerome J. *Introduction to Motion Based Design*. 1st ed. Prentice Hall, 2002. Print.

[31] Kareem, Ahsan, Tracy Kijewski and Yukio Tamura. "Mitigation of Motions of Tall Buildings with Specific Examples of Recent Applications", Wind and Structures, Vol.2, No.3, 1999. pp.201-251. Web. 15 Apr. 2012.
<http://www.nd.edu/~nathaz/journals/(1999)Mitigation_of_Motion_of_Tall_Buildings_with_Recent_Applications.pdf>

[32] Ilgin, H. Emre, and M. Halis Günel. "The Role of Aerodynamic Modifications in the Form of Tall Buildings Against Wind Excitation." *Middle East Technical University - Journal of the Faculty of Architecture*. 28 June 2007. Web. 26 Apr. 2012.
<http://jfa.arch.metu.edu.tr/archive/0258-5316/2007/cilt24/sayi_2/17-25.pdf>.

[33] Kausel, Eduardo. *Advanced Structural Dynamics*. Cambridge: Massachusetts Institute of Technology, 2009. Print.

[34] Yalla, Swaroop Krishna. "Liquid Dampers for Mitigation of Structural Response: Theoretical Development and Experimental Validation." Diss. University of Notre Dame, 2001.*Scribd.* 22 Nov. 2010. Web. 05 May 2012.
<http://www.scribd.com/doc/43564568/Yalla-PhD-Thesis>.

[35] Tait, M. J., A. A. El Damatty, and N. Isyumov. *The Dynamic Properties of a Tuned Liquid Damper Using an Equivalent Amplitude Dependent Tuned Mass Damper*. Rep. Canadian Society for Civil Engineering, 5-8 June 2002. Web. 5 May 2012.
<http://pedago.cegepoutaouais.qc.ca/media/0260309/0378334/SCGC-BON/Documents/ST099-Tait-Damatty.pdf>.

[36] Matta, Emiliano, and Alessandro De Stefano. "Robust Design of Mass-uncertain Rolling-pendulum TMDs for the Seismic Protection of Buildings." *Mechanical Systems and Signal Processing* 23.1 (2009): 127-47. *ScienceDirect*. Web. 6 May 2012.
<http://www.sciencedirect.com/science/article/pii/S0888327007001604>.